NTNU – Trondheim
Norwegian University of
Science and Technology

Condition Monitoring and Prognosis for Subsea Multiphase Pump

Fenfen Liu

Reliability, Availability, Maintainability and Safety (RAMS)
Submission date: June 2015
Supervisor: Anne Barros, IPK

Norwegian University of Science and Technology
Department of Production and Quality Engineering

RAMS
Reliability, Availability,
Maintainability, and Safety

Condition Monitoring and Prognosis for Subsea Multiphase Pump

Fenfen Liu

June 2015

MASTER THESIS

Department of Production and Quality Engineering

Norwegian University of Science and Technology

Supervisor: Professor Anne Barros

Preface

This report is a Master's thesis in the master programme of RAMS (Reliability, Availability, Maintainability and Safety) within the Department of Production and Quality Engineering at NTNU (Norwegian University of Science and Technology). It was carried out during the spring semester of 2015.

In February, 2015, my supervisor Anne Barros and me had a meeting with my future tutor in FMC Technology, Geir Werner Nilsen, to talk about my Master's thesis. Geir suggested me to write about the condition monitoring of subsea pumps as a case. Since multiphase pump is more advanced and new technology, I decided to research the condition monitoring of a multiphase pump to show how condition monitoring techniques are utilized for subsea equipment.

This report is written for the fifth-year RAMS students who have some knowledge of condition monitoring and the subsea production system.

Trondheim, 2015-6-10

Fenfen Liu

Acknowledgment

First of all I would like to express my great appreciation to my supervisor, Professor Anne Barros, for her patient guidance, enthusiastic encouragement and important feedback through the thesis.

I would also like to thank my future tutor in FMC Technology, Geir Werner Nilsen, who kindly suggested me to study the condition monitoring of subsea pumps for this thesis.

In addition, I would like to offer my thanks to the fellow students in the Condition Based Maintenance group, who often discuss with me about the condition monitoring topics, which helps me to have a clearer thinking of the thesis.

F.F.L.

Summary and Conclusions

This thesis presents a case study about the condition monitoring of the twin-screw multiphase pump in the subsea field to demonstrate how condition monitoring techniques can be applied for subsea equipment. Firstly a FMECA (Failure modes, effects, and criticality analysis) worksheet is carried out to identify the critical components of a twin-screw multiphase pump. Among the identified critical components, the mechanical seal and the twin screws are determined as study objects. For the condition monitoring of the mechanical seal, four different methods are introduced to detect the conditions of the mechanical seal. Then a physics-based model and a data-driven model are presented respectively as the diagnosis and prognosis models for the case of mechanical seals. For the twin screws, by learning the wear mechanism of the screws, the pressure distribution along the screw axis is decided to be measured to analyse the wear conditions of the twin screws. Afterwards Hidden Markov Model (HMM) is proposed for the failure diagnosis and prognosis. In addition a numerical example is computed to prove that HMM has the ability to identify the current wear state and predict the remaining useful life of the twin screws.

Contents

Chapter 1

Introduction

1.1 Background

During the last three decades, the application of subsea technologies have been developed significantly to the oil and gas production, which makes it possible to explore more reservoirs under deep sea. As more and more new technologies have been introduced to the subsea field, both the total number of subsea completions and the maximum water depth of subsea installations have increased dramatically.

Unlike the production equipment onshore or on a platform, the complex and unclear subsea environment bring various challenges to the maintenance activities. Usually the subsea maintenance requires a service vessel, Remote Operated Vehicle (ROV), specialized personnel, subsea tools,etc. Thus the preparatory work can be as long as one month before the repair is executed. In case of the occurrence of a critical failure that causes a sudden shutdown, the whole system may be idle for a long time until the preparation is done and the weather is favourable for maintenance activity, even though the real repair takes only several hours. The long idle time results also in the lower availability of the subsea system, which means huge economic losses and even worse reputation loss for oil and gas production industry.

Condition monitoring (CM) techniques have been introduced to solve this problem in the subsea field. By installing various sensors at the key points of the system, the condition data can be obtained and remotely monitored. With the application of signal process technology, the main features, namely, the health indicators of the machine, are extracted from the raw condition data, which provides a better view of the current condition of the system. Then advanced algorithms are utilized for failure diagnosis and remaining useful life prediction. The main advantage of CM is that it can help maintenance personnel to schedule maintenance activities in the most cost-effective way by giving an accurate judgement of the current condition of the system. Meanwhile the data collection phase can be continuously real-time that does not disturb the operation of the system.

Even though CM has been well developed in other areas such as railway and aerospace, subsea CM started just a few years ago. Most industries focus only on the monitoring of the flow process, including the flow pressure, temperature and flow rate, etc. But the equipment itself also needs to be monitored, for the degradation of the equipment would directly lead to the reduced efficiency of production. Since the subsea industry is a relatively young field, there are not plenty of literatures about the CM of subsea equipment. And most of them (e.g., Friedemann et al. (2008), Donnelly (2013)) provide only an abstract framework or concept of subsea CM rather than detailed practical information about how CM techniques are implemented for subsea equipment.

In this thesis a case study is carried out to present the procedure of CM for subsea equipment. In February, 2015, my supervisor Anne Barros and me had a meeting with my future tutor in FMC Technology, Geir Werner Nilsen, to talk about my Master's thesis. Geir suggested me to write about the CM of subsea pumps as a case. Since multiphase pump (MPP) is new developed boosting technology and is more advanced than conventional pumps, it would be more interesting to research the CM of MPP. Then I decided to use MPP as a case for subsea CM. MPP is able to pump the liquid and gas together, and the gas volume fraction could be as high as 95% for twin-screw MPP. Whereas the conventional pump can only pump liquid. Thus in the traditional solution, a separator is installed to separate the multiphase flow into gas and liquid, then the liquid is pumped by a conventional pump while the gas is compressed by a compressor. A single MPP is competent for the work done by a separator, a pump and a compressor together. Hence, MPP is more cost-effective.

For the CM of MPP, firstly a simplified FMECA (Failure modes, effects, and criticality analysis) is carried out to identify the critical components. Then the detailed CM information is demonstrated at component level for the critical components. For each certain component, the following questions need to be solved: which condition data are necessary for CM, which sensors can be utilized, how to measure the useful data, which models can be applied for failure diagnosis and prognosis.

1.2 Objectives

The main objective of this Master thesis is to carry out a case study about the CM of MPP to present how CM can be applied for subsea equipment. To realize this objective, the following sub-objectives have to be reached:

1. Learn about the current subsea condition monitoring techniques, and the general procedure of condition monitoring.
2. Find out the critical components of a multiphase pump.
3. Figure out which condition data are useful for condition monitoring, and how to measure them.
4. Figure out which models can be applied for the failure diagnosis and remaining useful life (RUL) prediction for different components.

1.3 Limitations

Due to the time limit and a lack of practical experience or information about multiphase pump, this thesis has the following limitations:

- In the FMECA of a twin-screw multiphase pump, not all possible failure modes have been analysed. Only the main failure modes for each component are listed in the worksheet. In addition, the ranking level for the failure frequency, detectability and severity of each failure mode have been simplified, which may make the results of the FMECA not so precise as a professional one.

- The condition monitoring for a whole system requires comprehensive knowledge about the details of each part in the system and sufficient practical experience as well, which is very difficult for a student without information from the practice. Thus the condition monitoring research is carried out only at the component level.

- Owing to time limit, it is impossible to research the condition monitoring techniques for all critical components identified. Only the mechanical seal and twin screws are studied as examples.

- The proposed physics-based model and proportional hazard model (PHM) for the mechanical seal are not verified with data due to a lack of real data in this case.

- For the wear of the screws, only Hidden Markov Model (HMM) is trained in Matlab to show its ability for diagnosis and prognosis, while Hidden Semi-Markov Model (HSMM) is not trained since it requires more advanced programming skills. Besides, due to a lack of real data, the data in the numerical example for HMM are generated optionally in Matlab, which cannot provide practical information for the real situation.

1.4 Approach

Firstly literature review has been done to learn about the whole subsea production system and the current subsea CM techniques. The detailed procedure of CM is also learned form the standard ISO 17359:2011. As a typical subsea equipment, the twin-screw multiphase pump is determined to be the study object. Then a simplified FMECA is carried out to identify the critical components, among which the mechanical seal and twin screws are further studied. For the mechanical seal, a physics-based model and a data-driven model are introduced based on literature review to predict the RUL. For the twin screws, HMM is proposed to estimate the current wear state and predict the RUL. Additionally a numerical example is computed to verify the ability of HMM for both diagnosis and prognosis. The training data for the example are generated optionally in Matlab owing to a lack of real data.

1.5 Structure of the Report

The rest of the report is organized as follows:

- Chapter 2: Describe the current problems for subsea equipment, and introduce the development of CM both in other areas and in subsea field. The challenges of CM in subsea field are also stated. Then the detailed procedure of CM is presented.

- Chapter 3: Based on the system structure analysis of the twin-screw multiphase pump, a FMECA worksheet is carried out at the component level, and the critical components are identified.

- Chapter 4: The CM for the mechanical seal is described in details, including the existing monitoring techniques, the important condition data and the corresponding measurements. In addition a physics-based model and a data-driven model are demonstrated for the RUL prediction.

- Chapter 5: Present how CM is applied for the wear of the screws. Then HMM is proposed for the failure diagnosis and prognosis. In addition a numerical example is taken in Matlab to prove HMM is able to identify the current wear state and predict the RUL as well.

- Chapter 6: Present the summary and conclusions for this thesis, and then propose recommendations for the further work.

Chapter 2

Condition Monitoring in Subsea

2.1 Problem Description

The application of subsea technology to reservoir development has been widely accepted as an oil production solution, since it provides more opportunities to explore the reservoirs under deep water. During the past three decades, there has been a significant development in subsea field. Both the total number of subsea completions and the maximum water depth of subsea completions installed have increased dramatically, which is shown in Figure 2.1.

However, the availability of subsea equipment is usually lower than topside machinery, and some studies show that availability of subsea assets can be as low as 90% (Langli et al. (2001)). Availability is commonly defined as

$$Availability = \frac{MTBF}{MTBF + MTTR}$$

where MTBF is mean time between failures (or uptime), and MTTR is the mean time to repair (or downtime). The lower availability of subsea equipment is mainly caused by large value of MTTR rather than MTBF. MTTR consists of both preparation and execution time of maintenance activities. On a deck of a platform, it does not take a long time for preparation, since personnel, tools and spare parts are usually already available. While in a subsea system, the maintenance requires a service vessel, Remote Operated Vehicle (ROV), specialized personnel,

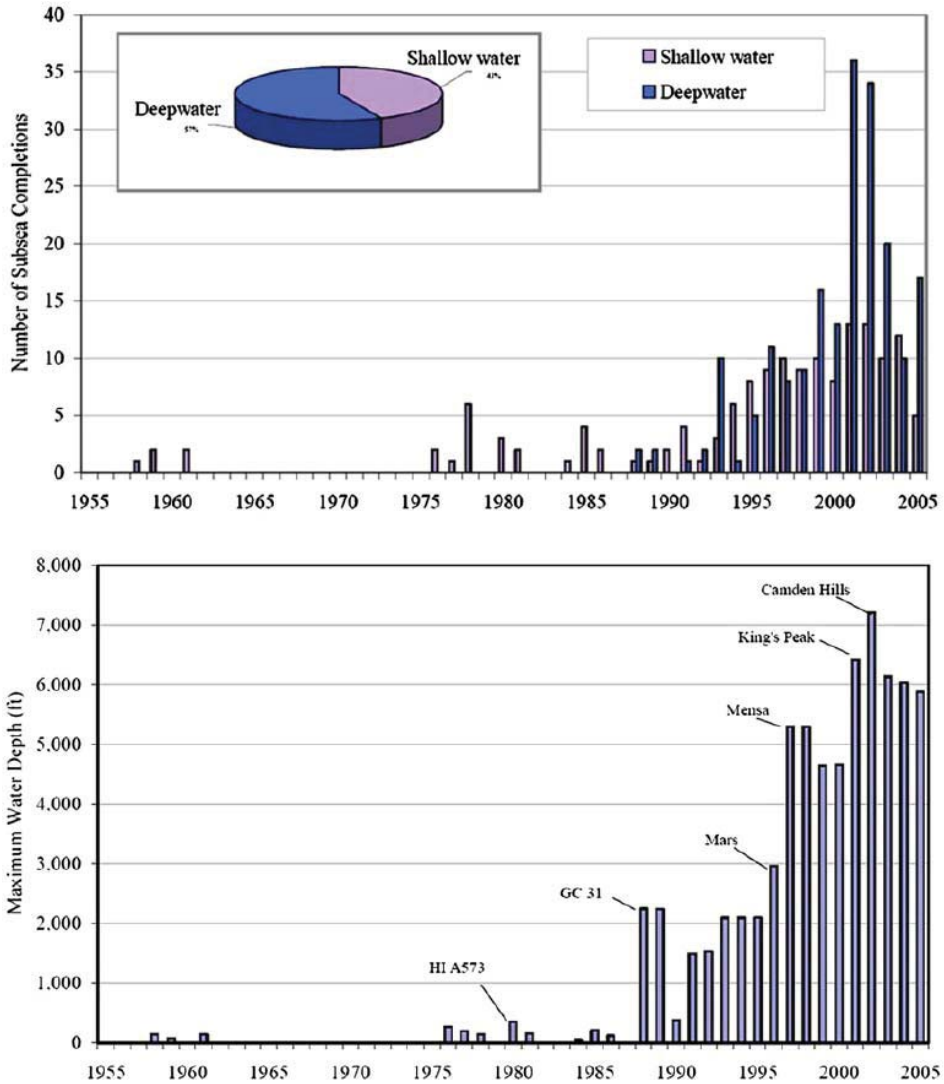

Figure 2.1: The total number of subsea completions and the maximum water depth for subsea installations (from Bai and Bai (2012))

and subsea tools, which is also coupled with other factors such as weather conditions that have to be favourable for the maintenance (Bencomo (2012)). For instance, the actual replacement of a subsea pump module typically takes 24 hours, while the preparation time can be as long as one month (Eriksson et al. (2014))

One feature of subsea industry is that the occurrence of unplanned shutdown will cause huge economic losses that is usually beyond the acceptable level. Hence, it is very important to keep a high availability of subsea equipment to avoid or reduce the undesired shutdown of the system. Apparently if the preparation time can be effectively reduced, the availability is expected to be higher. If the potential failure can be accurately predicted before it occurs, the preparatory work can start earlier, so that no extra preparation time is taken when maintenance activity is required. For the prediction work, condition monitoring (CM) is an effective method. The way how CM can be applied to improve availability is shown in Figure 2.2. Therefore subsea condition monitoring is a path to increased availability and increased recovery in the reservoir.

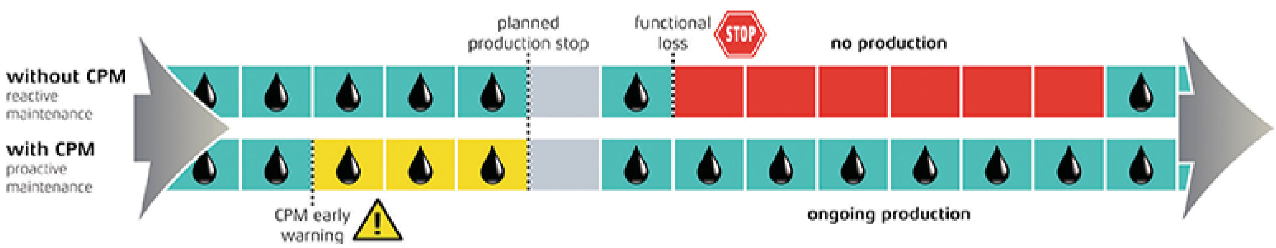

Figure 2.2: Difference with and without a condition and performance monitoring (CPM) system (from Donnelly (2013))

2.2 Development of Condition Monitoring

Before CM began to be used in subsea, it has been successfully developed in other industries. In maritime industry, it is profitable to keep the vessels in transit as much as possible. Thus condition based maintenance (CBM) is introduced to minimize the repair time at ports. One important development in maritime industry is the creation of Technical Condition Index (TCI), which is a measure for integrity, health and performance based on aggregation of technical, financial and statistical parameters (Bencomo (2012)). TCI uses Bayesian network to describe the behaviour of a hierarchical system. All the TCIs are computed from the lowest component level (child) to the top level (parent) to determine the impact of the child nodes to the parent node, thus finally providing a top level status for the whole system. The computation can be simply described as:

$$TCI_{parent} = \frac{\sum_i^n TCI_i * w_i}{\sum_i^n w_i}$$

where TCI_i is the TCI of child i, w_i is the weight of child i, and n is the number of child nodes. The main advantage is that TCI provides information about the system as a whole rather than just only as a list of conventional key performance indicators for individual components, which helps to understand the whole system status.

In railway industry, the degradation and malfunctions of the trains could reduce the transport efficiency and cause economic losses. In worse situation, it would lead to catastrophe with serious human injuries and fatalities for passenger trains. Hence, it is very necessary to utilize CM techniques to detect the early warnings of possible failures to avoid train accident. Due to the special mechanics in trains, the railway has developed new methods of CM for locomotives, bogies and railways. For instance, the infrared technology is applied to detect high temperatures in wheels and bearings, acoustic bearing detectors are installed to record sounds from bogies, vibration analysis for bearing defects, and strain gauges and accelerometers are used to measure lateral and vertical forces to estimate the risk of derailment and defects on wheels (Lagnebäck (2007)). Some of these CM techniques have been gradually used in other areas for machinery diagnosis.

In power generation industry, the power production is greatly influenced by the price of commodities and energy demand. It is reasonable to operate at high capacity when the energy demand is high, and vice versa. In addition, the power generation should be always available since the consumption is uninterrupted, which requires the power plants with very high reliability level. For this reason, CM techniques in power generation industry concentrates mostly in diagnosis and failure prediction, and advanced algorithms have been introduced to keep a good balance between the supply and demand, such as neural networks and expert systems (Bencomo (2012)). The application of advanced algorithms made a great improvement for the diagnosis and prognosis in CM techniques. The main advantage is that the new algorithm can make a prediction based on both historical and current data, which is more accurate than the conventional computation that is only based on historical data.

Aerospace has developed the most advanced CM owing to the obvious safety reasons. Adaptive Gaussian Threshold (ATA) algorithm has been created as a novel method for failure detection when historical information is scarce. It is able to recognize new behaviour patterns that were not considered during the modelling of machine failure (Bencomo (2012)). Another improvement is that relevant software has been programmed for CM techniques, providing failure diagnosis, trending prediction and decision support, which makes the application of CM techniques more convenient.

Even though subsea systems have existed for more then 50 years, it was only a few years ago that oil and gas companies have considered CM for subsea equipment as an essential part of their asset management strategies. In 2009 General Electric (GE) established the Subsea Monitoring and Remote Technology Center (SMARTCenter). In this CM system, condition data are collected at the field by various sensors, then the remote fault diagnosis , equipment performance trending and recommendations for maintenance intervention are carried out on-line. The main objectives of SMARTCenter are to detect hydraulic leakage, umbilical resistance degradation, chock erosion, and valve signature (Bencomo (2012)). Schlumberger offers a parallel surveillance system that can monitor the Christmas tree, risers, flowlines and jumpers, detect the leakage, and measure temperature distribution for hydrate prediction. FMC has developed a Condition and Performance Monitoring (CPM) system for subsea CM. It monitors electrical and mechanical components continuously and provides real-time processing to determine current operating conditions and early detection of degradation. It researches also some advanced CM technologies such as optoelectronic leak detection, which is able to detect very small leakage.

As a relatively new industry, it faces a couple of challenges with respect to CM in subsea field:

- Lack of specialized CM equipment (both hardware and software) for subsea applications due to the short history of the subsea industry.
- Due to the complex environment under deep water, many conventional sensors are not competent to collect data stably.
- Most conditions monitored in subsea field are only the flow process data, but very few information about the conditions of the subsea equipment has been recorded and stored.
- Many subsea installations are located far away from the shore, which makes it difficult to access the equipment. The calibration, upgrade and maintenance of CM equipment become also difficult and expensive.

2.3 Procedure of Condition Monitoring

The standard ISO 17359:2011 provides a detailed CM procedure as shown in Figure 2.4. To be simplified, the procedure can be divided into five parts: system identification, data acquisition, data processing, diagnosis and prognosis, decision making, which is shown in Figure 2.3.

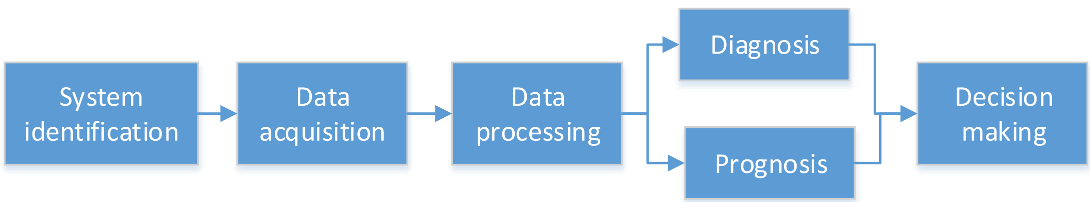

Figure 2.3: Simplified procedure of condition monitoring

System identification is to analyse the system function of the study object, identify the possible failure modes both on the system and component level. Then the critical components have to be figured out for CM. Besides, the information about the existing historical data and available research methods needs to be collected for the sequent work.

Data acquisition is to collect useful condition data and event data. Before the implementation of data acquisition, the following problems have to be solved: which data have to be measured and recorded, how to measure condition data, what type of sensors can be utilized, the location and number for different sensors, how signal is sent from sensors to the controller.

Data processing is necessary when the raw data cannot be directly used. Usually the measured raw data contain a lot of noises from the environment. So the first step of data processing is the remove the irrelevant noises, which is called filtering. In many situations, even the filtered data cannot provide a straightforward view of the current system status. Thus further data processing techniques are applied to extract features that can be used as indicators of the system performance. For example, Fast Fourier Transform is widely used to extract the frequency features from time-domain data, since the amplitudes of the frequencies have the ability to indicate different failure modes for a component such as bearing.

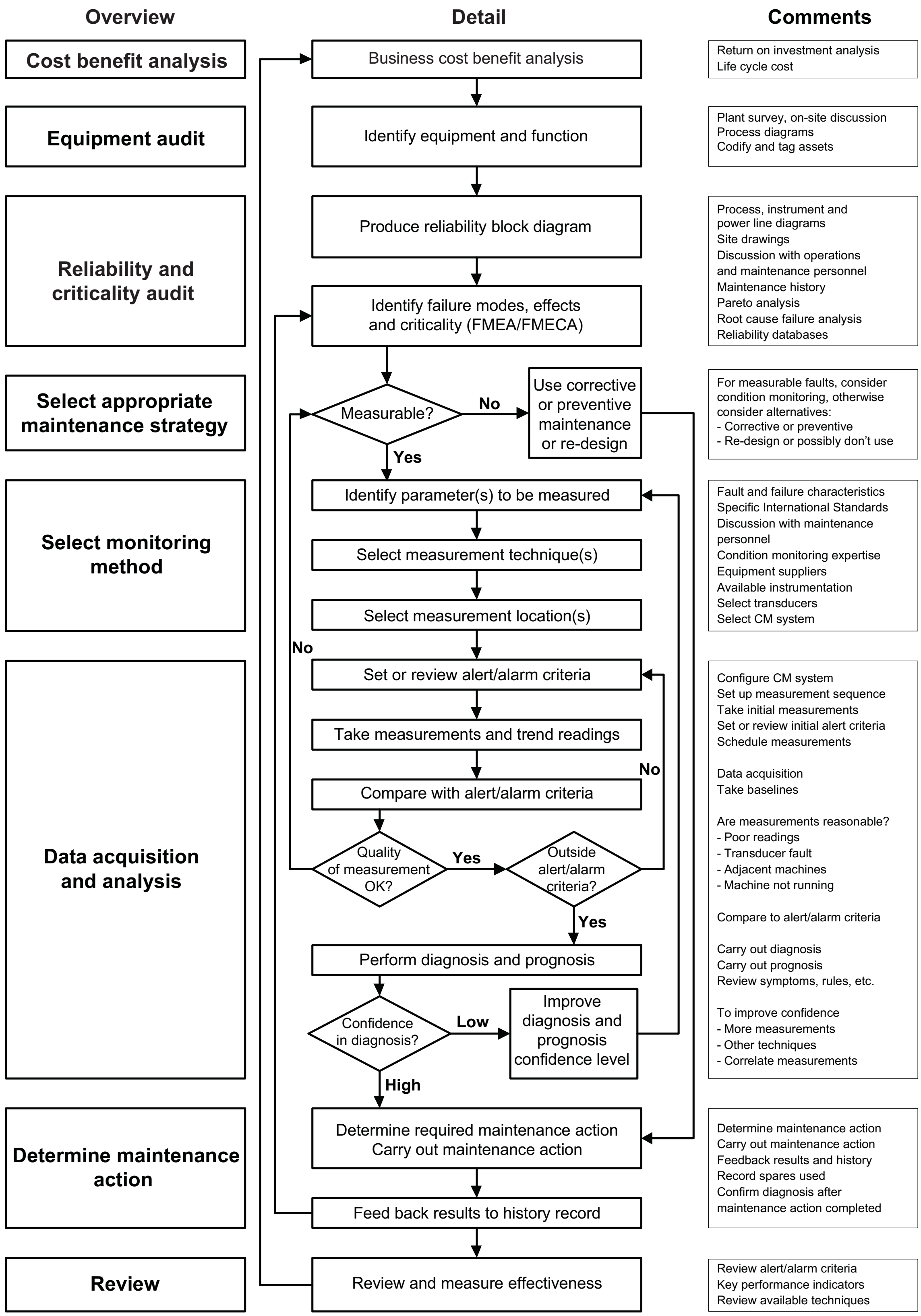

Figure 2.4: The flowchart for implementing a condition monitoring programme (from ISO (b))

Diagnosis

Diagnosis is executed based on the feature extraction, aiming to determine the presence, position and severity of the defect or damage in the machine. Nowadays the concept of machine diagnosis is computerised comprising automated detection and classification of faults.

ISO 13379-1:2012 (ISO (a)) divides current diagnostic approaches into two types: data-driven approaches and knowledge-based approaches. The basic idea of both of them is to build a base model which describes the normal conditions of the machine either based on data or based on knowledge, and then look at the difference between the real measured value and the estimated value from the base model. If the difference is too large and beyond the acceptable range, then it may reveal that there is something wrong in the machine. In opposite, if the difference is within the acceptable range, it shows that the machine is healthy so far.

Data-driven approaches establish mathematical models to fit the data obtained from machine. These models do not represent the physical mechanism of the machine. The data used could be event data or condition data or both. Event data includes which kind of failures happened at what time, when and where the replacement or repair activities were carried out, etc., while condition data are measured to indicate the health conditions of the machine or components.

Knowledge-based approaches are mostly based on the deep knowledge of the working mechanism of the machine and the experience of the technicians. These approaches also use event data and condition data, but not so much as data-driven approaches.

Prognosis

In practice, machinery prognosis can be explained as the forecast of the remaining useful life (RUL), future condition, or probability of reliable operation of an equipment based on the acquired condition data. The mail difference between diagnosis and prognosis is that, diagnosis is usually carried out after the appearance of a symptom or a suspicious anomaly to judge whether this is a fault or abnormal behaviour,where it is, and how serious it is, while prognosis is to predict the future behaviour of the machine, e.g., when the next failure will happen, the probability that the system will fail before the next inspection, etc. Prognosis is developed based on diagnosis.

In the situation of expensive shutdown or catastrophic consequences, it is very important to apply prognostics to predict the expected time to failure or the probability that the system can survive a future period, thus corresponding actions will be decided to prevent undesired consequences. With accurate prognosis, it is expected to significantly reduce expensive downtime, spares inventory, maintenance labour costs and hazardous conditions (Heng et al. (2009)).

The basic objective of prognosis is to predict the future behaviour of machine. Before CBM was adopted, there were many traditional methods to estimate the reliability of the machine. According to the different types of data used for prediction, Heng et al. (2009) group the existing methods for predicting rotating machinery failures into three categories: traditional reliability approaches based on event data, prognostics approaches based on condition data,and integrated approaches based on both event and condition data.

Decision Making

The ultimate objective of diagnosis and prognosis is to provide support for maintenance decision making. For general degradation process, there are three decision rules based on the result of diagnosis and prognosis, as explained in the bellow.

Define the involved parameters as:
L - predetermined failed level;
M - the maintenance level at which necessary maintenance activity is needed, obviously $M < L$;
T_m - the minimum of the tolerable time to failure;
Q - the maximum of the tolerable probability of failing within one preventive maintenance (PM) interval;
$\hat{x}(k\tau)$ - the estimated degradation level at the kth interval.

Rule 1: If $\hat{x}(k\tau) < L$ and $\hat{x}(k\tau) > M$, then carry out PM.
Rule 2: If $\hat{x}(k\tau) < L$ and the mean remaining useful life at time $k\tau$ $mean\, RUL(k\tau) < T_m$, then carry out PM.
Rule 3: If $\hat{x}(k\tau) < L$, and the probability of failing within one PM interval $P_r(RUL(k\tau) \leq \tau | T >$

$(k-1)\tau) > Q$, then carry out PM.

With various prognostic models, the degradation level expression $\hat{x}(t)$ and the survival function $R(t)$ can be estimated based on the condition data and the event data. Thus it is convenient to calculate

$$mean\,RUL(t) = \frac{1}{R(t)} \int_t^{\infty} R(x)\mathrm{d}x,$$

and

$$\begin{aligned} P_r(RUL(k\tau) \leq \tau | T > (k-1)\tau) &= 1 - P_r(RUL(k\tau) > \tau | T > (k-1)\tau) \\ &= 1 - R(k\tau | T > (k-1)\tau), \end{aligned}$$

and further include the degradation level information as below, which makes the prediction of the probability more accurate.

$$\begin{aligned} P_r(RUL(k\tau) \leq \tau | T > (k-1)\tau, X(k\tau) = x(k\tau)) &= 1 - P_r(RUL(k\tau) > \tau | T > (k-1)\tau) \\ &= 1 - R(k\tau | T > (k-1)\tau, X(k\tau) = x(k\tau)) \end{aligned}$$

Apparently Rule 2 and Rule 3 are more advanced than Rule 1, because they take into account the stochastic properties of the degradation process in the future, while Rule 1 does not. However, in fact Rule 1 is the most commonly used in many industries since it is much easier to be managed. Besides, when the data is not sufficient enough, Rule 3 is preferred rather than Rule 2, as the calculation of the probability has much less variance than the calculation of $mean\,RUL(t)$.

Despite of the results of diagnosis and prognosis, maintenance decision making is also influenced by many other factors, such as the economic costs, maintenance strategy, regulations and laws, the availability of spare parts and specialized tools, human resources, etc. Hence, a robust maintenance decision making system is needed to balance the different profits and boundaries.

Chapter 3

FMECA of Multiphase Pump

3.1 The Application of Multiphase Pump

Pumps are widely used in subsea to improve the efficiency of oil production by keeping the requisite pressure in the flowline. Conventional pumps can only be used to pump liquid-dominated flow due to that they are originally designed to pump liquid. However, the crude oil from production wells usually contains a high fraction of gas, which cannot be pumped directly by conventional pumps. A common solution to this problem is to use a scrubber to separate the gas and liquid, then pump and compressor are used in parallel to handle the separated liquid and gas respectively. Afterwards the gas and liquid are recombined and sent in a common flowline to shore, as shown in Figure 3.1.

As new technology develops, multiphase pump (MPP) has been gradually applied in subsea during the last three decades, aiming to help to eliminate separators, compressors, and individual pumping equipment, thus increasing the oil production at lower costs(Schoener (2004)). In comparison with conventional pumps, the main advantage of MPP is its ability to handle the flow with a high gas volume fraction (GVF), e.g., as high as 95~98% in inlet conditions, which means a single MPP is able to complete the total work of a scrubber, a conventional pump and a compressor. Besides, owing to the high integrity of the MPP, it uses much less space than the solution in Figure 3.1 and is much easier to be installed. Moreover the flexibility of a MPP to handle both low pressure and high pressure conditions makes it an ideal tool to develop marginal

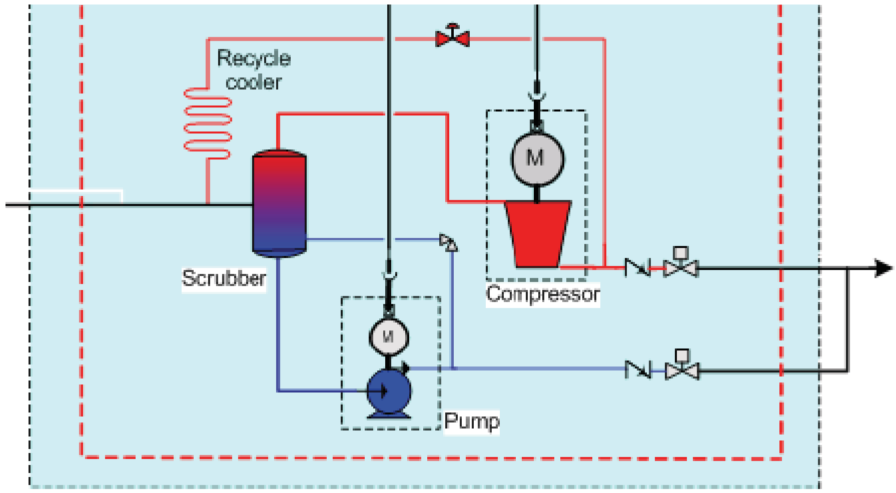

Figure 3.1: Solution with conventional pump (from Eriksson (2010))

fields.

There are several different types of MPP, as shown in Figure 3.2. Both positive displacement pumps and helico-Axial pumps have been successfully used in onshore, offshore or subsea field. The most commonly used is the positive displacement, twin-screw MPP. Therefore a twin-screw MPP is selected as a research object for condition monitoring.

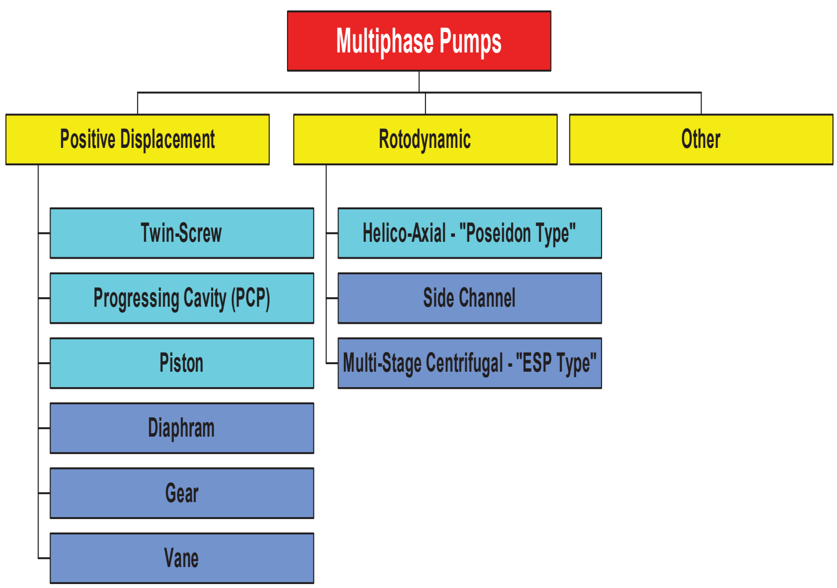

Figure 3.2: Classification of multiphase pump (from Scott et al. (2004))

For MPP is relatively new technology, most researches still focus on the design of MPP. Thus plenty of experiments have been carried out to analyse or model the performance of a new MPP under various operating conditions. For example, Prang and Cooper (2004) analyses the flow rate influencing factors, including gas volume fraction (GVF), liquid viscosity, rotational speed, screw geometry, pressure rise, etc. Scharf (2006) uses experiments to show that twin-screw MPP with declining pitch has better performance than the one with normal pitch. Kim et al. (2015) illustrates how to use design of experiments(DOE) techniques to improve MPP performance. Feng et al. (2001) constructs a model to simulate the multiphase pumping process based on energy conservation and mass conservation principles. Egashira et al. (1998) calculates the theoretical amount of backflow in twin-screw MPP. Only few literature introduces the condition monitoring system of MPP, e.g., Rohlfing (2010), but it is just conceptual to some extend rather than practical application. As such an important boosting equipment in subsea oil production, the CM for MPP would sooner or later be a topic. Therefore this thesis focuses on how CM can be applied to improve the availability of MPP, including which critical components need CM, which data need to be collected, which sensors are utilised, and which models can be used for diagnosis and prognosis based on the collected data.

3.2 Introduction of FMECA

FMECA (Failure modes, effects, and criticality analysis) is a methodology to identify and analyse all potential failure modes of the various parts of a system, the effects these failures may have on the system, and how to avoid the failures or mitigate the effects of the failures on the system (Rausand (2013)). In addition, by ranking the severity, frequency and the detectability of each failure mode, FMECA can identify which failure modes are critical that need more attention. In this way, FMECA provides a basis not only for maintenance planning, but also for quantitative reliability and availability analysis.

There are two approaches to FMECA: bottom-up approach and top-down approach. The bottom-up approach is used when a system concept has been decided. FMECA is carried out on the component level that the failure modes of each component are studied one-by-one. Thus it is also called hardware approach. To the contrary top-down approach is mainly used in an early design phase before the whole system structure is decided. FMECA is carried out on the system or sub-system level. It focuses mainly on system or sub-system malfunctions instead of the exact component failure. In this case, since the MPP is already well designed and manufactured, bottom-up approach is applied, thus FMECA of MPP is carried out at the component level.

There are mainly five steps to work on FMECA:

1. FMECA prerequisites, including the object of study, the objectives, which approach is preferred, the plan of the FMECA procedure and relative working team, etc.

2. System structure analysis. Usually the system is divided into sub-systems and further into component level.

3. Failure analysis and preparation of FMECA worksheets. Based on the system structure analysis, all possible failure modes of each component are listed in the FMECA worksheet. The ranking of the severity, frequency and detectability of each failure mode need to be clearly identified.

4. Team review. This step focuses on the related risk of each failure mode to assess whether the risk is acceptable. If it is unacceptable, improvement measures have to be proposed to reduce the risk until it is within the acceptable level.

5. Corrective actions. Improvements are executed based on the team review.

The main advantage of FMECA is that it is a very structured and reliable method for evaluating hardware and systems, and the concept and application are easy to learn. The system structure analysis makes it easy to evaluate complex systems. However, the disadvantage is that the FMECA process may be very time-consuming, and it is easy to forget human errors in the analysis.

Since the main objective of FMECA in this case is to identify the critical components that need condition monitoring, the part of how to avoid the failures or mitigate the effects of the failures on the system is removed from the FMECA worksheet. Step 2 and 3 are presented in details.

3.3 System Structure Analysis

As shown in Figure 3.3, a twin-screw MPP mainly consists of four parts: pump unit, slug distributor, GLCC (Gas Liquid Cylindrical Cyclone), and recirculation system. Firstly the oil produced from the production well is transferred through the inlet line into the combination of the slug distributor and the pump unit. Then it goes to the cyclonic column of GLCC through a tangential inlet, which can form a vortex to roughly separate gas and liquid. In recombination column gas and liquid are recombined to the common outlet line and sent out. The recirculation system recirculates a small part of liquid from the bottom of recombination column to the pump suction to ensure a minimum of liquid in the multiphase mixture.

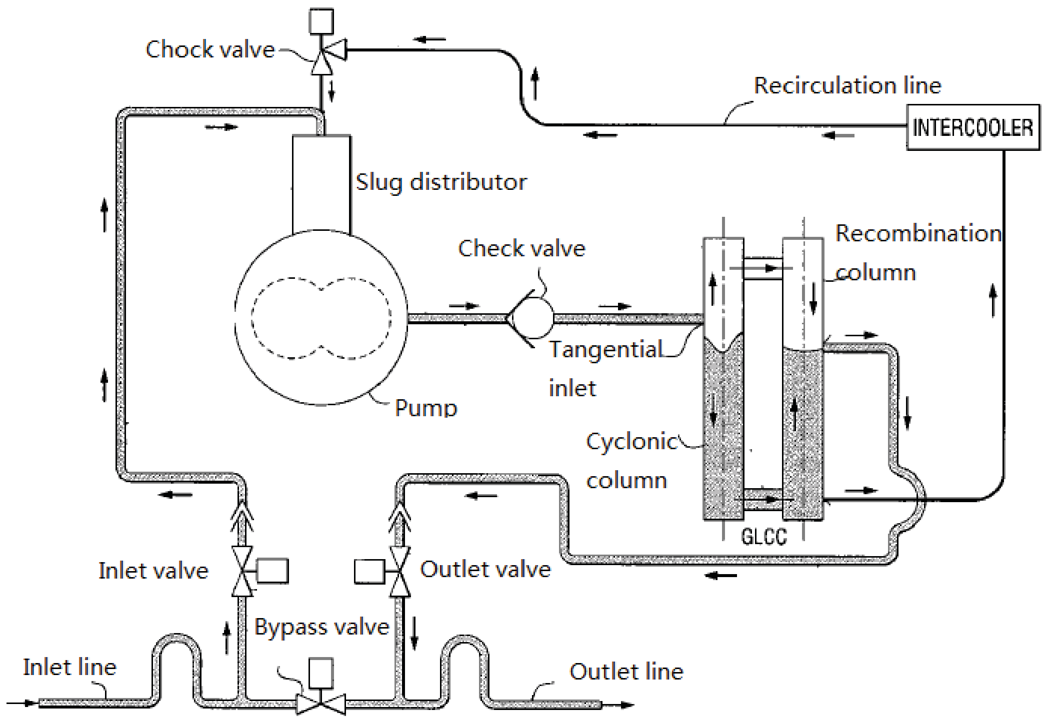

Figure 3.3: A simplified overview of a twin-screw multiphase pump (adjusted from Campen et al. (2009))

Pump unit

The basic structure of a twin-screw MPP is shown in Figure 3.4. The other side of the driving shaft is a combination of motor and gearbox. During operation, the rotation of the two screws can provide the requisite pressure to pump the multiphase flow from suction to discharge port.

Even though a twin-screw MPP can deal with as high as 95% GVF condition, the problem is that there must be a minimum of liquid in the multiphase mixture (e.g., 5%) to maintain a seal between the screw flanks and the screw tips and casing(Campen et al. (2009)). If the minimum of liquid is not met in multiphase service, the MPP cannot pump the flow but still continues to rotate. Even a short period of this kind of idle running could cause the overheating of pump, and afterwards leads to shutdown of the pump when the high temperature is sensed by the temperature sensors. Hence, the alltime minimum of liquid is a prerequisite for the continuous operation of the MPP. To solve this problem, a common method is to recirculated a small part of liquid from the discharge of MPP to the suction to ensure the liquid minimum. It is proved to be an effective method even though it reduces the capacity of the pump to some extend. To decrease the negative influence of liquid recirculation, a chock valve is installed in the recirculation line to control the flow rate of recirculated liquid according to the GVF of the flow in the suction, as shown in Figure 3.3.

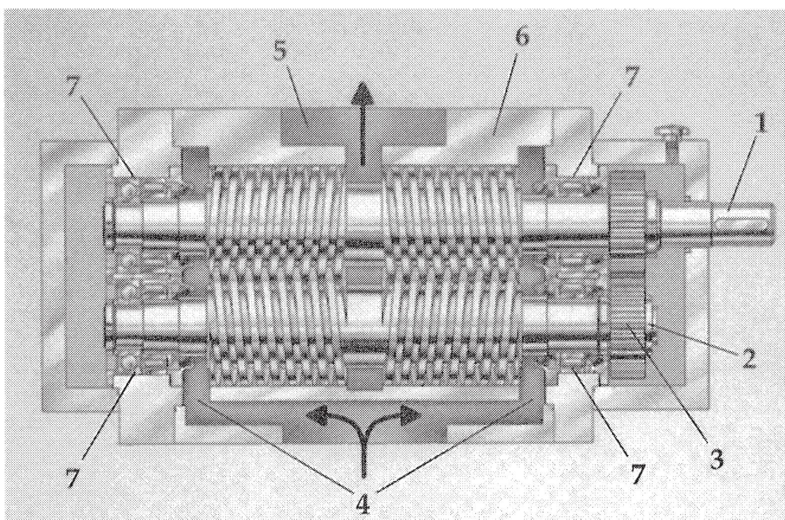

Figure 3.4: The inside structure of a twin-screw pump (1.Driving shaft; 2.Driven shaft; 3.Gear; 4.Suction; 5.Discharge; 6.Housing; 7.Bearing) (from Vetter et al. (2000a))

GLCC

The main objective of GLCC is to briefly separate gas and liquid to provide the liquid for recirculation. If there was no GLCC, the recirculated flow (directly from the discharge port of pump) would contain a part of gas. When the gas enters the suction of pump from the recirculated line, the lower pressure in the pump would lead to the expansion of the gas, thus reducing the volume of suction flow and correspondingly the capacity of the pump. In even worse situation, if the suction flow happens to be a single phase of gas, the recirculated flow is also full of gas, then the pump begins to run idly. Since there is no liquid discharged to take away the heat in the pump, the temperature would continuously increase until the pump stops due to overheating.

The application of GLCC can effectively solve these problems. The tangential inlet of the cyclonic column can help to form a vortex of the flow to separate gas and liquid. Afterwards the gas and liquid are recombined through the recombination port on the recombination column and sent out through the common outlet pipe. The recirculation port is located at the bottom of the recombination column, which ensures recirculated flow is all liquid. In addition, the liquid connection of the cyclonic column and the recombination column makes a U-tube effect, which means the liquid level in the latter is always the same with the liquid level in the former. When the liquid level is below the recombination port, the output is only gas while liquid is stored in GLCC. Therefore, in the case of full gas suction, the stored liquid in the recombination column can still be recirculated to ensure the continuous operation.

Recirculation system

The recirculation system simply consists of a recirculation port at the bottom of the recombination column, recirculation line, an intercooler and a chock valve. In front of the recirculation port, there is a vertical baffle plate fixed on the bottom of the recombination column, aiming to prevent the majority of particulates from entering the recirculation line. Thus the particulates in the flow will not be repeatedly recirculated in the whole system, which is able to decrease the corrosion and erosion. The intercooler in the recirculation line is used as a fluid resistor to reduce the discharge pressure to the level of the pump suction pressure it will be "meeting"(Campen et al. (2009)). A chock valve is installed with the same purpose.

Slug distributor

In a multiphase pipeline, it produces normally "slug" flow, that is a liquid-gas two-phase flow and represented by alternating volumes of gas and liquid. Since the conditions keep changing in the pumping process, there is high uncertainty of the gas slugs in the crude oil. And the gas-dominated slugs could cause a similar situation to a lack of the minimum amount of liquid. Thus a slug distributor is applied to deal with it. The inside structure of a slug distributor is shown in Figure 3.5.

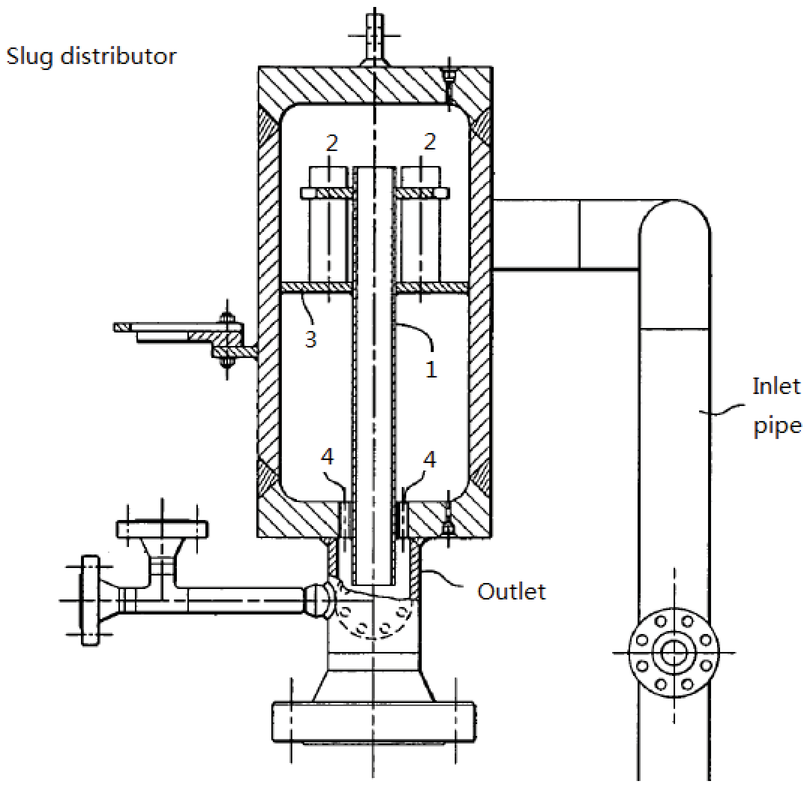

Figure 3.5: The inside structure of a slug distributor (1.Standpipe; 2.Breather tube; 3.Perforated plate; 4.Metering holes) (adjusted from Campen et al. (2009))

The inlet of the slug distributor is also a tangential inlet to form a vortex to separate the gas and liquid. Since the standpipe and the breather tubes are higher than the inlet port, the gas passes through the standpipe, while the liquid flows through the holes in the perforated plate into the down space. The gas existing under the perforated plate can go back to the up space through the breather tubes, and then passes through the standpipe to the outlet. There are six metering holes in the bottom of the slug distributor, which is to lead the liquid from the down space to the outlet. At the outlet port, the gas from the standpipe and the liquid from the metering holes are recombined to the pump unit. In this way, the gas-dominated slug could be eliminated.

Based on the description, the system structure is represented in Figure 3.6.

3.4 FMECA Worksheet

The FMECA of the twin-screw MPP is taken at the component level. Referring to Rausand (2013), the detection ranking, failure rates classification, and the severity classes, defined in FMECA, are simplified and adjusted according to the practical information of a MPP, for the main purpose of the FMECA here is to identify the critical components that need to be monitored.

The detailed FMECA worksheet is shown in Appendix B. The failure rate of each failure mode

Table 3.1: The defined detection ranking. (Adjusted from Rausand (2013))

Rank	Description
1	Very high probability that the defect will be detected. Verification and/or controls will almost certainly detect the existence of a deficiency of defect.
2	High probability that the defect will be detected. Verification and/or controls have a good chance of detecting the existence of a deficiency/defect.
3	Moderate probability that the defect will be detected. Verification and/or controls are likely to detect the existence of a deficiency or defect.
4	Low probability that the defect will be detected. Verification and/or control not likely to detect the existence of a deficiency or defect.
5	Very low (or zero) probability that the defect will be detected. Verification and/or controls will not or cannot detect the existence of a deficiency/defect.

Table 3.2: The defined failure rate ranking. (From Rausand (2013))

Rank	Class	Description
1	Very unlikely	Once per 1000 years or more seldom
2	Remote	Once per 100 years
3	Occasional	Once per 10 years
4	Probable	Once per year
5	Frequent	Once per month or more often

refers to the data from *OREDA Offshore Reliability Data 5th Edition* (SINTEF (2009). In the last

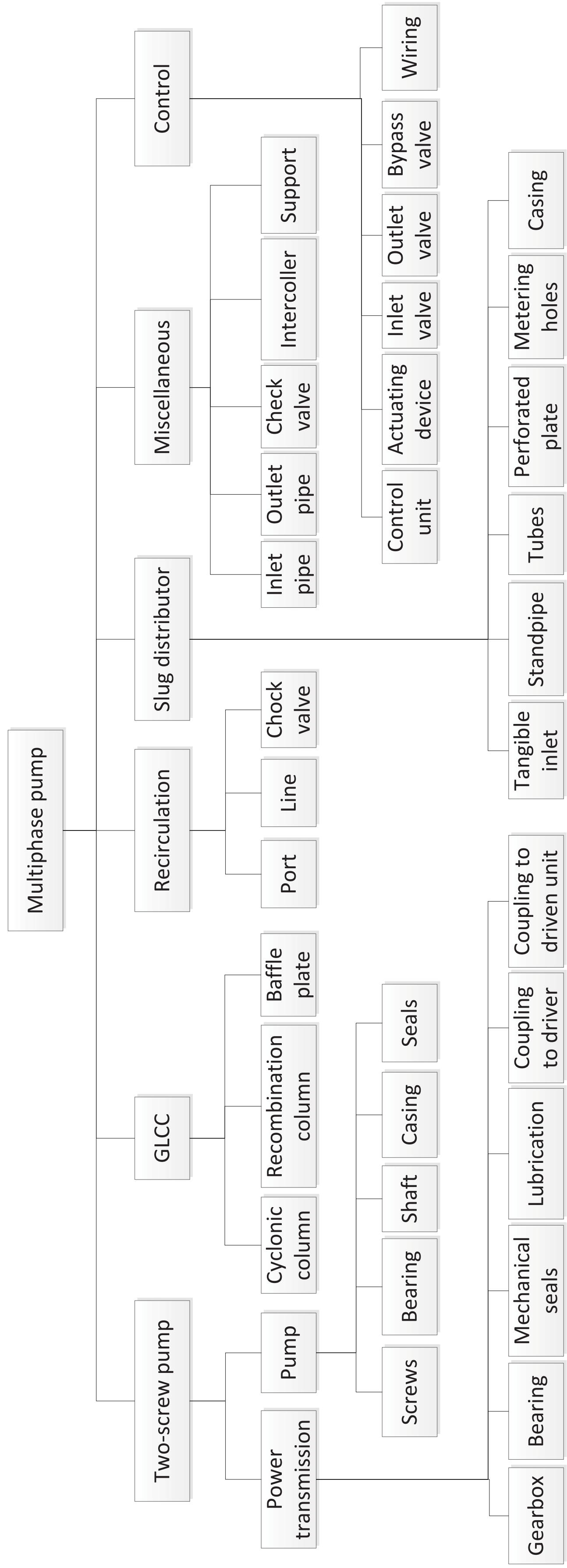

Figure 3.6: System structure of the twin-screw multiphase pump

Table 3.3: The defined severity ranking.

Rank	Description
5	Failure results in the stop of the pumping system, and may cause serious damages to the equipment.
4	Failure results in serious reduction of the efficiency of the pumping system.
3	Failure results in moderate reduction of the efficiency of the pumping system.
2	Failure results in a little reduction of the efficiency of the pumping system.
1	Failure does not currently results the reduction of the efficiency of the pumping system. But with time going, it may have negative influence in the operation process.

column of the worksheet, RPN, means Risk Priority Number, which indicates the level of criticality of each failure mode. Here RPN is defined as

$$RPN = D \times F \times S$$

where D is the detectability of failure, F is the failure rate, and S is the severity ranking for the consequences of the failure modes. The higher the RPN is, the more critical the failure mode is. Therefore, a critical failure mode usually has the following characters: difficult to be detected, high failure frequency, and serious consequences. According to the result of FMECA, the following components can be identified to be critical, because some of their failure modes have relatively high RPN: gearbox, twin screws, bearing, mechanical seals, control unit and valves. Owing to the time limitation and space boundaries, only mechanical seals and twin screws are selected as examples to show how condition monitoring can be applied for the MPP in subsea field.

Chapter 4

Condition Monitoring of Mechanical Seals

Based on the result of FMECA in Chapter 3, the mechanical seal is a critical component that may cause the system down when it fails. This result is alike to many other literatures, for example, Anderson et al. (2002) mentions that turbo-machinery breaks down mainly because of a mechanical seal failure. Therefore it is necessary to monitor the conditions of the mechanical seal to detect the early signs of potential failures, thus avoiding the undesired shutdown of the pumping system.

In a twin-screw MPP, there are four mechanical seals installed on each side of the two screw shafts, aiming to prevent oil leakage from the pump chamber. The external leakage through the mechanical seals will lead to the reduced pressure in the pump chamber, which could decrease the capacity of the MPP sharply. Moreover, severe friction of the mechanical seals may cause the overheat situation and the vaporization of the oil and water around, which would result in over-pressure and even shutdown of the MPP. Due to the limitation conditions of the maintenance in subsea field, the maintenance activity usually needs a long time to prepare before it can be implemented, e.g., one month. Hence, it is vital to monitor the conditions of the mechanical seals to provide necessary information for preventive maintenance.

Besides, considering the crude subsea working environment, the mechanical seals of a MPP face many challenges, e.g., the high quantity of sand, dry running without enough lubrication liquid in a certain case, high fluid viscosity, highly variable and unpredictable pressure, changing operation speed(Evans and Janssen (2002)). And external environment of mechanical seals is the general deep-water subsea environment. The condition monitoring of mechanical seals will not only support the preventive maintenance scheduling, but also provide valuable information for the designers to overcome these challenges.

4.1 The Structure of a Mechanical Seal

A mechanical seal is developed to seal the rotation part of a machine, e.g., shaft. It consists of five basic components: a stator, a rotor, a spring, an O-ring between the stator and the housing, another O-ring between the rotor and the shaft, as shown in Figure 4.1.

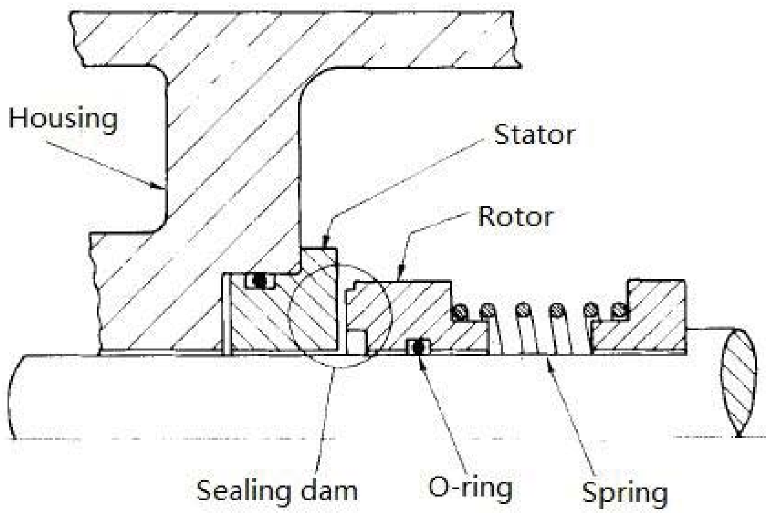

Figure 4.1: Schematic of a mechanical seal (adjusted from Ruddy et al. (1982))

The stator is fixed on the housing, aiming to prevent the contact between the rotor and the housing. If there was no a stator, the friction during the operation will damage the housing, which is very difficult and expensive to be replaced or maintained. While it is quite convenient to replace the stator. The O-ring between the stator and the housing can prevent the leakage through the stator. The spring forces the rotor to be close to the stator face, thus avoiding the large clearance caused leakage between the stator and rotor. The rotor is fixed on the shaft, so it is rotating with the shaft during operation. The other O-ring prevents the leakage between the rotor and the shaft. Due to the spring, the rotor is slidable in the axial direction, while the rotor can also have a radial displacement owing to the cushion working of the O-ring. In this way, the movement of the rotor can compensate the vibration and movement of the shaft in the axial and radial direction.

During operation, the clearance between the stator and the rotor would be filled up with fluid, thus forming a fluid film, that is an essential part of a mechanical seal. The fluid film separates the stator and the rotor from each other to eliminate the contact of the two faces. If the fluid film fails, the contact of the stator and rotor would lead to deformation and overheat of the mechanical seal. Moreover the high temperature can cause even worse thermal deformation. Therefore frequent contact would reduce the lifetime of a mechanical seal quickly. It could be beneficial if the fluid film is liquid, since it can be both lubrication and cooling medium. However, in a MPP the pumped fluid could be 100% gas in some situations. To maintain a full and stable liquid film, one solution is to input a small part of the recirculated liquid from the recirculation system (introduced in Chapter 3) into the mechanical seal. In this situation there would be an entrance and an exit respectively for the lubrication liquid.

One may doubt that the clearance between the stator and the rotor could cause leakage, and this is true. Hence, the problem is to keep an ideal thickness of the liquid film so that the contact friction is avoid, meanwhile the leakage is negligible. Generally there would be little leakage when the machine starts up and stops. However during normal operation, the pressure and the viscosity in the liquid film could prevent leakage.

Since the features of the liquid film and other parameters of the sealing dam reveal the most operation conditions of a mechanical seal, a great many of efforts are taken by researchers to monitor the working conditions in this area. For instance, the most widely measured parameters are the thickness of the liquid film, temperature, pressure, etc.

4.2 The Existing Condition Monitoring Methods

For a mechanical seal, the failure is either excessive wear by contact friction or leakage due to large clearance between the seal faces. Therefore there are mainly two directions for the condition monitoring of a mechanical seal: contact detection and leakage detection. For different purposes, different parameters are selected to be measured. This section introduces four existing condition monitoring methods for mechanical seals: thermal method, measurement of rotor displacement, acoustic emission technique, and ultrasonic technique.

4.2.1 Thermal method

Thermal method focuses on the temperature of the seal faces, that is influenced by the original fluid temperature, the viscous and flow rate of the fluid, and the contact friction between the two faces. Compared with the heat generated by the contact friction, the former two factors' influence is usually negligible. Hence, thermal method mainly aims to monitor the seal faces contact by detecting the apparent temperature increment. The quantity of the increased temperature can indicate the severity of the contact.

Another application applies to the mechanical seal with an extra lubrication supply. Two temperature sensors are installed in the entrance and exit of the lubrication liquid respectively to measure the input and output liquid temperature. In addition a flowmeter is used to measure the flow rate of the lubrication liquid. With the temperature increment, flow rate, and the physics features of liquid (e.g., density, viscosity), the increased quantity of heat can be calculated and is approximately the heat generated by the contact friction, which can be regarded as an indicator of the severity of the contact as well(Holenstein et al. (2000)).

Thermal method is very easy to be implemented, and is a very direct way to detect the contact situation. However, before the two seal faces contact each other, there is no way to monitor the trend of the decreased liquid film. Therefore the thermal method is only used for diagnosis, with very limited space for prognosis. Besides, even though temperature is a very important parameter for the mechanical seals performance, it is too unilateral to judge the overall conditions of a mechanical seal. Thus other measurements must be supplemented.

4.2.2 Measurement of rotor displacement

Owing to the spring and the O-ring, the rotor can have displacement both in the axial and radial directions in relative to the shaft. Yamauchi and Inoue (1994) introduces a condition monitoring method by simply measuring the axial and radial displacement of the rotor. The positions of these sensors are shown in Figure 4.2. The displacement sensor could be an eddy-current sensor or an optical sensor.

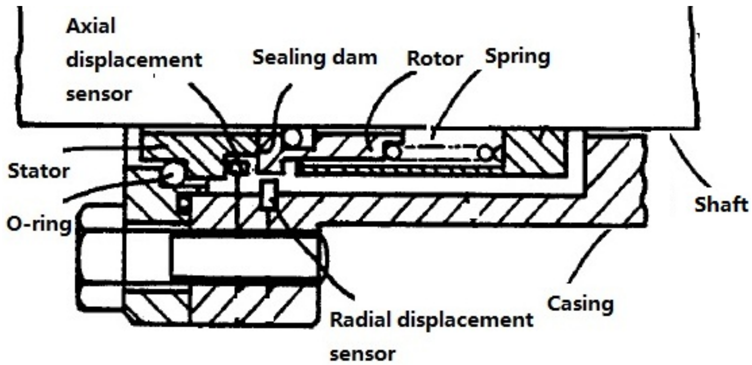

Figure 4.2: Positions of the displacement sensors (adjusted from Yamauchi and Inoue (1994))

Radial displacement of the rotor

The radial displacement sensor is fixed in the inner side of the casing and it is adjacent to the outside of the rotor. By recording the changing distance between the surface of the sensor and the outside of the rotor, the radial displacement of the rotor is calculated. Since the rotor is rotating together with the shaft, its radial displacement should be a periodic variables. Thus the radial displacement sensor generates a periodic signal waveform. Under normal operation, the condition of the liquid film is stable, and the waveform of the radial displacement is also stable and smooth. While if the clearance between the seal faces becomes either too small or too large, the features of the waveform will change correspondingly.

A signal processor is applied to analyse the features of the waveform. One basic signal processing method is to transfer the time-domain signal into frequency-domain information by Fast Fourier Transform(FFT). To detect the contact of the seal faces, a frequency analysis can be taken to look into the frequencies of the minimum and maximum amplitude of the waveform. When the clearance reduces gradually, the frequencies of both the minimum and maximum amplitude increases subsequently. When the value of the frequency reaches the threshold, the contact happens. In this way, the contact situation can be predicted by tracking the increasing trend of the frequencies of the minimum and maximum amplitude of the waveform.

Another signal processing method is envelope analysis of the waveform amplitude. The envelope of the signal is extracted by picking up the values of the maximum amplitude. When the clearance of the seal faces becomes larger and larger, the envelope will go down accordingly. Again there should be a threshold level to judge whether the leakage happens. Thus the leakage can be predicted through the trend of the envelope and the velocity it decreases.

Axial displacement of the rotor

An axial displacement sensor is installed on the stator in front of the sealing dam to detect the displacement of the rotor in the axial direction. Since the stator is fixed on the housing, the axial displacement of the rotor is the most direct indicator for the size of the seal faces clearance. When the distance between the rotor face and the sensor is increasing, the size of the clearance is increasing as well. In contrast, a decreasing distance means the clearance is getting smaller. Hence, it is quite convenient to detect the contact or leakage.

Even though the analysis of axial displacement is much easier than the radial displacement, Yamauchi and Inoue (1994) shows that the radial displacement is more effective to predict the leakage in the earlier stage. As shown in Figure 4.3, the amplitude of the radial displacement begins to decrease very early, while the in the axial direction it increases not so long before the leakage. There is a much longer degradation period for the radial displacement than the axial one. Therefore it is more effective to predict the leakage through the analysis of radial displacement.

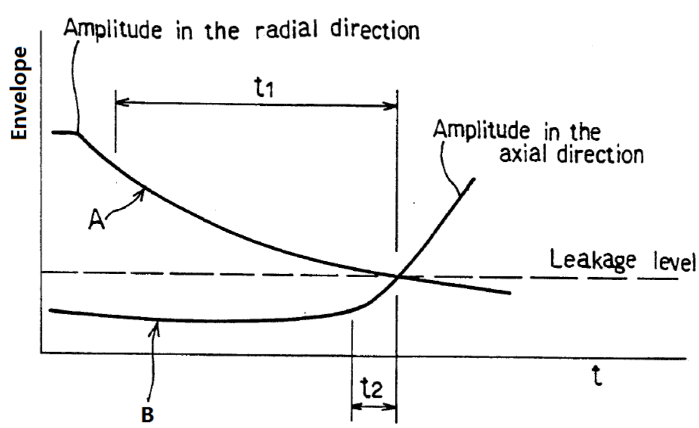

Figure 4.3: The envelope of the amplitude of the radial and axial displacement (from Yamauchi and Inoue (1994))

It is easy to implement the rotor displacement measurement. The signal processor must have the ability to extract the valuable information from the original signals. The main advantage is the potential of prognosis to detect the contact or leakage at an early stage, if the changing trend of the main frequencies and amplitudes can be well estimated mathematically. However it has the same drawback with the thermal method, that is the displacement of the rotor is not enough to evaluate the overall performance of the mechanical seals.

4.2.3 Acoustic emission technique

Acoustic emission (AE) technique is theoretically similar to vibration analysis. They both detect the sound response of the rotating components, and complex signal processing is necessary to figure out the features that contain the health information of the components. The difference between them is that AE technique is more sensitive to the subtle changes in the signal than vibration analysis. For instance, the vibration signal can be measured up to the frequency range 30-50 kHz, while the AE is able to manage the frequency range up to 50-400 kHz (Rus et al. (2007) and Mba et al. (2006)). Therefore the AE technique is more available to monitor the slight changes in the liquid film conditions.

AE was used to detect the friction of the faces of a mechanical seal as early in 1993 (Huang et al. (2014)). Like vibration signals, the AE signals contain abundant information of the conditions and performance of mechanical seals. However, due to the limitation of the signal processing technology and the computer processing speed, the development of AE technique is not fast. Another important disadvantage of AE is that in practice it is usually very difficult to distinguish the AE signals of mechanical seals from the signals of other rotating components, e.g., gear, bearing. However in laboratories, AE technique is repeatedly tested and proved to be effective to monitor the condition of mechanical seals, e.g., Huang et al. (2014), Mba et al. (2006), Zhang et al. (2014).

A piezoelectric sensor is widely used as an AE sensor, and it is installed at the back of the stator, as shown in Figure 4.4. The signals generated by the AE sensor are sampled at a higher frequency, e.g., 1 MHz, to ensure that all important information is collected. Since the original AE signals contain many noises, it needs to be filtered for the subsequent signal analysis. Afterwards the time-domain signal is usually transferred into frequency-domain by FFT to get a spectrum of the signal, in which the amplitude of each frequency constituent gives a good indication for the anomaly of the mechanical seal. For instance, an abnormally high amplitude of one specific frequency constituent generally indicates a mechanical malfunction. Other than FFT, Zhang et al. (2014) mentions another time-frequency analysis method to deal with the non-linear non-stationary signal processing, e.g., AE signal produced by a mechanical seal. The method is called Empirical Mode Decomposition (EMD). The main advantage is that the EMD results have clear physical meaning, giving a more clear way to diagnose the performance of a mechanical seal.

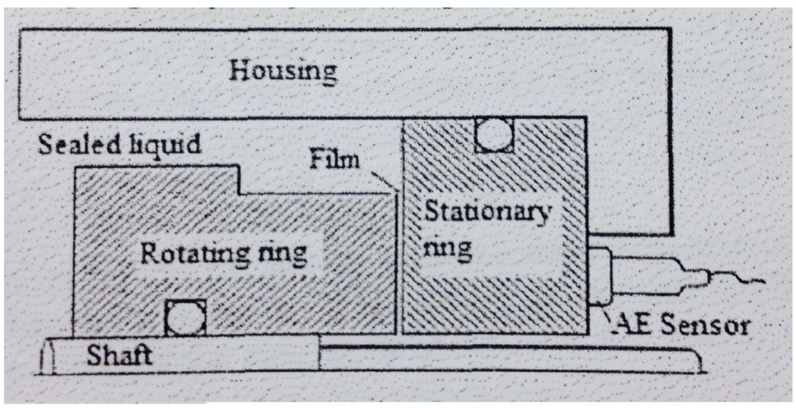

Figure 4.4: The position of an AE sensor (from Huang et al. (2014))

The most commonly measured AE parameters are amplitude, root mean square(RMS), and energy (Mba et al. (2006)). The amplitude of AE signal is directly related to the energy released while contact friction occurs. RMS measures the average power in AE signal, which can show the overall noisy level and is an indicator of the unbalanced conditions of rotating parts. Thus if the mechanical seal occurs misalignment, contact or deformation, the value of RMS will be out of normal range. The energy in AE signal is also en indicator for the occurrence of contact friction.

In addition to diagnosis, AE technique has a large space for developing prognosis. Because AE is very sensitive to the subtle effects from the early stage. If the trend of the amplitude, frequencies or other features can be well estimated, it can effectively predict the occurrence of the contact friction, the mechanical degradation, the changes of the liquid film, and possible leakage as well.

The implementation of AE technique is not difficult, but it needs a high-capacity signal processor to effectively distinguish the different AE signals from different rotating components. Since AE signal contains a large amount of unclear information, the main challenge is how to deal with these AE data to figure out useful information. One advantage of AE technique is its ability to reflect the overall performance of a mechanical seal. So far AE technique is mostly tested to monitor the contact situation of the mechanical seals. However, with the development of signal processing technology and the capacity of the computer, AE technique is still a promising method for both diagnosis and prognosis of a mechanical seal.

4.2.4 Ultrasonic technique

Due to the main drawback of AE technique that it is difficult to distinguish between mechanical seal AE signals from those of other sources, the ultrasonic technique is widely researched to monitor the conditions of the mechanical seals. And it is proved to be able to not only detect the occurrence of contact friction, but also estimate the thickness of the liquid film before contact.

The principle of ultrasonic technique is based on the different propagation characteristics of ultrasound in different mediums. The liquid film between two seal faces can be simply regarded as a liquid layer between two solid bodies. When the ultrasound goes through them, the reflection depends on the ultrasonic frequency, the acoustic properties of the liquid and solid, and the layer thickness (Dwyer-Joyce et al. (2003)). Since the ultrasonic frequency is predefined, and the acoustic properties of the liquid and solid can be obtained based on the materials, the geometries, or experiments, it is available to calculate the thickness of the liquid layer according to the reflection of the ultrasound.

When applying the ultrasonic technique in monitoring a mechanical seal, one piezoelectric transducer is attached to the back of the stator, as shown in Figure 4.5. Unlike the AE sensor just passively monitors the AE from the mechanical seal, the ultrasonic transducer actively generates ultrasonic waves with known frequency and amplitude, and then receives the reflected ultrasound from the seal faces. In other words, it is used both as an ultrasound source and receiver. For the features of the ultrasound are already known, the waves can be easily distinguished from other noises and emissions, thus overcoming the disadvantage of AE technique

(Anderson et al. (2000)). During normal operation, the ultrasound propagates toward the seal faces, then only a negligible part of wave is incident into the liquid, and the most part is reflected. However, when contact happens, the solid rotor acts as a transmission path for the ultrasound. As a result, the reflection is apparently reduced, as well the reflected wave amplitude decreases, which can be easily detected as a sign of the contact.

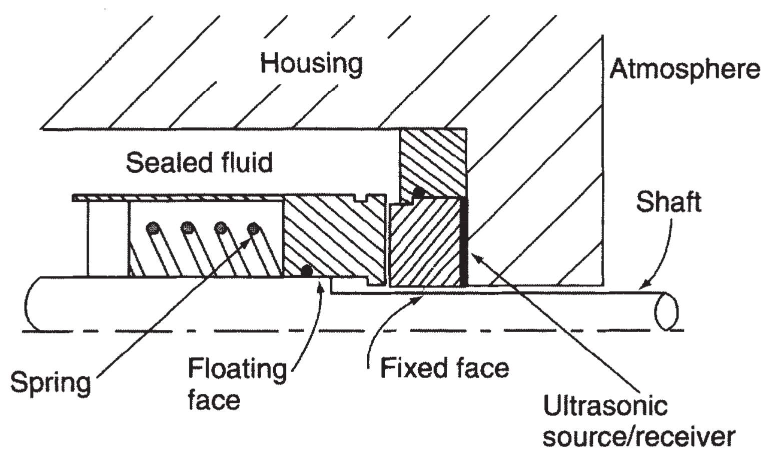

Figure 4.5: The position of an ultrasonic sensor (from Anderson et al. (2002))

To estimate the liquid film thickness, physics equations about the propagation, reflection and incidence of ultrasound should be applied, meanwhile the frequency and material combination of the mechanical seal have to be taken into account. Usually the liquid film thickness is very thin, e.g., at μm level, then the liquid layer behaves like a spring and the reflection of the wave depends on the spring stiffness. Thus the proportion of reflected wave is related to the thickness of the liquid film by using a quasi-static spring model. This method has a high requirement of the transducer's accuracy, as errors as low as 5% could have a significant effect on the calculated film thickness (Reddyhoff et al. (2006)).

Ultrasonic technique is more precise in measuring the film thickness than other methods. It needs also a signal processor to analyse the reflected wave and compare it with the originally generated signal, but it is not so complicated as the AE technique. One practical issue for ultrasonic technique is that the transducer is very sensitive to the temperature variation. Thus alternative piezoelectric materials should be investigated. Overall, with accurately estimated liquid film thickness, it is possible to predict both seal faces contact and leakage.

4.2.5 Comparison between different methods

As shown in Table 4.1, these four methods are compared in the following aspects: type of sensors used, type of data collected, the main purpose of the method, the potential for prognosis, the advantages and disadvantages respectively. In general, the thermal method is applicable when only a rough detection of contact situation is needed. The easiest way to detect both contact and leakage is to measure the displacement of the rotor in axial and radial directions, but the result may be not so precise. If other mechanical malfunction is of interested, for example, the misalignment, wear, deformation, crack, acoustic emission technique is more effective than others. Ultrasonic technique monitors the conditions of the mechanical seals by measuring the film thickness, which is highly dependent on the knowledge of ultrasound propagation, and it has high requirements of the sensors.

Another point is that from the view of data type, only thermal method measures the operating data, while other methods all select to measure the performance data of the mechanical seals to diagnose the conditions. Obviously the performance of the mechanical seals is significantly influenced by different operating conditions and boundaries, e.g., the pressure around the seal, the speed of the shaft, the work load, the flow rate, etc. However, few of them are taken into account to predict the future performance of the mechanical seals. Perhaps the performance data is enough for diagnosis, but it would be more interesting to establish a prognosis model which combines both operating and performance data.

4.3 Diagnosis and Prognosis Models

As discussed in Section 4.2.5, the performance data (film thickness and the acoustic emission) is highly influenced by the operating data, for example, the temperature of the seal faces, the speed of the shaft, the pressure around the mechanical seals (Reddyhoff et al. (2006)), the entry and exit temperature of the lubrication, the flow rate, and the viscosity of the liquid (Holenstein et al. (2000)). If the relationship between the performance data and the operating data could be figured out and described in a mathematical way, it would be very useful for both diagnosis and prognosis.

Table 4.1: The comparison between different methods

Methods	Thermal Method	Displacement method	Acoustic emission	Ultrasonic
Sensor type	Temperature sensor	Eddy-current sensor	Piezoelectric sensor	Piezoelectric sensor
Data collected	Temperature of the seal faces; Temperature of the input and output lubrication liquid	Axial and radial displacement of the rotor	Acoustic emission from the mechanical seal	Reflected ultrasound from the seal faces
Data type	Operating data	Performance data	Performance data	Performance data
Purpose	Detect contact situation	Detect both contact and leakage situations	Mainly detect contact	Measure liquid film thickness to predict the contact and leakage
Ability of prognosis	Very limited	Some potential	High potential	High potential
Advantages	Easy to be applied	Easy to be applied; Subsequent signal analysis is not complicated	Abundant information of the mechanical seal conditions; Be able to diagnose other types' mechanical malfunction	It is easy to detect the reflected waves from other noises; High accuracy in measuring the film thickness
Disadvantages	Unilateral information of the seal performance	Accuracy is not very high; Unilateral information of the seal performance	It is difficult to distinguish the seal AE signals from other noises; Signal processing is highly complex and time consuming	High requirements of the sensors

The basic idea is to establish a model that presents the relationship between the performance data and the operating data under the healthy conditions of the mechanical seal. In other words, given the values of the relative operating data, the model is able to estimate the reasonable performance of the mechanical seal when it is healthy. Meanwhile, the real performance data is measured through AE or ultrasonic technique. Then the estimated performance and the real one are compared. If the difference between them is within the acceptable range, then there is no problem for the mechanical seal. Otherwise it indicates the anomaly may occur. For instance, the model can be presented as

$$\hat{P} = f(x_1(t), x_2(t), x_3(t), ...)$$

where $\hat{P}$ is the estimated performance of a healthy mechanical seal when given the values of operating data. And it could be either the liquid film thickness or a feature value of the acoustic emission. $x_1(t), x_2(t), x_3(t), ...$ are relative operating parameters, e.g., temperature, pressure, speed of shaft respectively. Then two thresholds, the contact threshold L_c and the leakage threshold L_l, should be predetermined based on experiences and experiments. Afterwards, the diagnosis process is shown in Figure 4.6, where P is the measured real performance, and $D = P - \hat{P}$ is the difference.

As shown, this is quite a simplified diagnosis process flow, only considering three working conditions of the mechanical seals. In application it can be adjusted to be more detailed and specified for the target failure modes and working conditions. At the last step of the process flow, if the value of D is out of any defined range, there must be something wrong with the analysis system or the model. Hence, it needs to be corrected and modified.

For prognosis, the most important point is to figure out how the performance of a mechanical seal changes with time under the effects of various parameters, such as material, geometries, and operating parameters. Thus the performance should be modelled as a function of time and other parameters to predict the future trending. There are mainly two types of prognosis models: physics-based model and data-driven model.

Physics-based model assumes that an accurate mathematical model can be constructed from

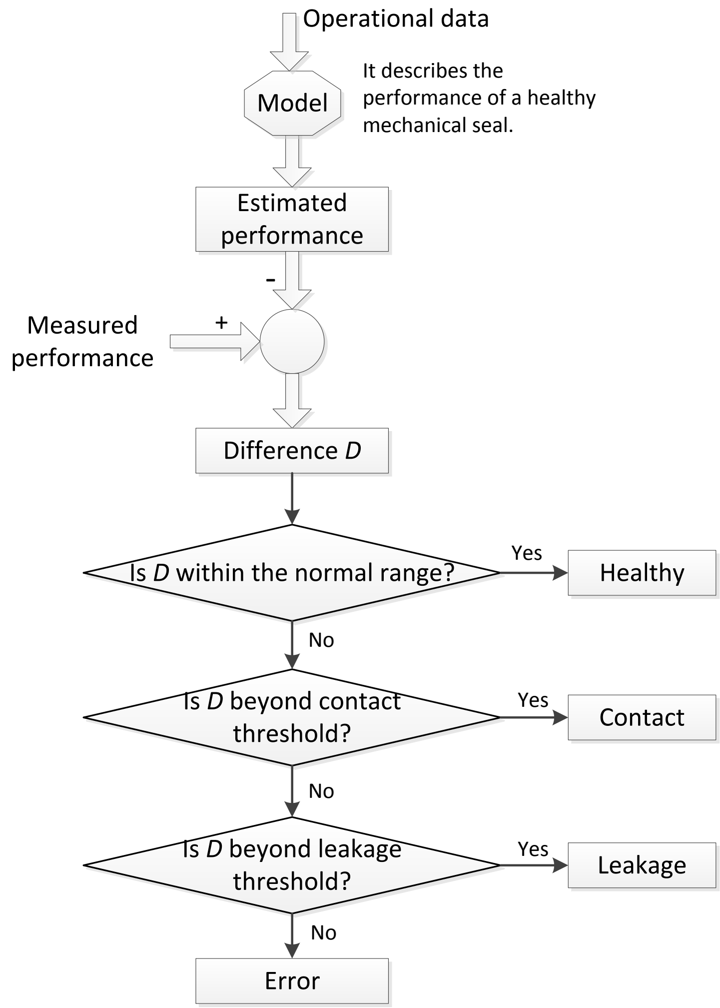

Figure 4.6: The basic idea of the diagnosis process flow

first principles (Dragomir et al. (2009)) to describe the physical characteristics of the system or failure modes. Hence, it needs well-rounded physical knowledge of the monitored components or system. The advantage is that once the model is constructed, it does not need too much data to verify the model. While the disadvantage is that sometimes the operating situation is too complicated to find available physical formulas to present it. In the mechanical seal case, it is necessary to apply the knowledge of hydromechanics, thermodynamics, mechanics, etc. to construct such a model.

Data-driven approaches drive models directly form collected condition data or event data or both instead of building models based on comprehensive system physics and human expertise (Heng et al. (2009)). Condition data includes the raw condition data and the associated covariates that are extracted from original data, such as temperature, pressure, amplitude and frequency of acoustic or ultrasonic signal. Event data means the records of the installation, maintenance and failure calender time. With a data-driven model, there is no need to know the failure initiation mechanism exactly. However a large amount of data is necessary to ensure an accurate model.

4.3.1 Physics-based model

The operation of a mechanical seal involves three major physical processes: the film lubrication process, asperity contact, and the thermal/mechanical deformation of the seal faces (Ruan et al. (1997)). These three processes are interacted with each other. Ruan et al. (1997) and Salant and Cao (2005) develops a physical model that takes into account these three processes to predict the liquid film thickness and the leakage rate.

This physical model is based on the following assumptions:

1. The seal is axisymmetric. Even though mechanical seals cannot be perfectly axisymmetric during operation, generally the hydrodynamic pressure caused by nonaxisymmetric face features could be negligible. Thus only the hydrostatic pressure is assumed to be present in the film.

2. During normal operation the seal is stable with equilibrium.

3. The thermal and mechanical deformation is small enough to be approximated as a linear function of the thermal and mechanical loads. In addition, the temperature change is assumed to be linearly dependent on the thermal load.

4. Since the liquid film is thin, it is assumed that there is no temperature change across the film, and the film and face temperatures are the same.

Asperity contact analysis

During equilibrium operation, the stable liquid film should keep the rotor relatively stationary in axial direction. Thus the net axial force on the rotor face is zero, e.g., the opening force equals to the closing force in magnitude but opposite in direction:

$$F_{closing} = F_{opening} \tag{4.1}$$

The closing force is produced by the sealed pressure and the spring force, and is given by

$$F_{closing} = p_s \pi((r_o)^2 - (r_i)^2) + F_{spring} \tag{4.2}$$

where r_o, r_i are the outer and inner radius respectively, p_s is the sealed pressure. For a given seal design and geometry, the closing force is a constant and is easy to determine, since p_s can be measured by a pressure sensor, and F_{spring} is calculated by the stiffness and the deformation of the spring. The opening force consists of the pressure force in the film and the contact force due to asperity contact, that is

$$F_{opening} = F_{pressure} + F_{contact} \tag{4.3}$$

where the pressure force depends on the fluid pressure distribution on the seal face:

$$F_{pressure} = 2\pi \int_{r_i}^{r_o} pr\,\mathrm{d}r \tag{4.4}$$

where r is the radial coordinate, and p is the fluid pressure. Similarly the contact force depends on the contact pressure distribution. Given a film thickness distribution, for a simple plastic asperity deformation, the contact pressure p_c is assumed to be a Gaussian asperity distribution:

$$p_c = H \int_h^{\infty} \frac{1}{\sigma\sqrt{2\pi}} e^{-z^2/2\sigma^2}\,\mathrm{d}z \tag{4.5}$$

where H is the flow stress, h is the film thickness, σ is the combined standard deviation of the surface roughness, and z is the axial coordinate. Thus the contact force is

$$\begin{aligned} F_{contact} &= 2\pi \int_{r_i}^{r_o} p_c r \mathrm{d}r \\ &= 2\pi H \int_{r_i}^{r_o} \int_{h}^{\infty} \frac{1}{\sigma\sqrt{2\pi}} e^{-z^2/2\sigma^2} r \mathrm{d}z \mathrm{d}r \end{aligned} \quad (4.6)$$

Film lubrication

The fluid mechanics of the lubricating film is governed by the Reynolds equation:

$$\frac{\partial}{\partial r}(r h^3 \frac{\partial p}{\partial r}) = 12\mu r \frac{\partial h}{\partial t} \quad (4.7)$$

where μ is the viscosity of the fluid, t is the time, and h is the specified film thickness at each location and instant of time. This equation is integrated in space and in time to yield the pressure distribution at each instant of time, which determines the leakage rate Q:

$$Q = \frac{\pi r h^3}{6\mu} \frac{\partial p}{\partial r} \quad (4.8)$$

The solution of Equation 4.1 - 4.8 needs the knowledge of the film thickness h that is a function of time t and radial coordination r. The film thickness is determined by the mechanical and thermal deformations, which will be discussed later.

Temperature

The thermal deformation and the temperature are influenced by the heat generated at the two seal faces. The heat generation rate per unit area at node j is given by

$$Q_j = [\frac{\mu\omega^2 r^2}{h}]_j + [f\omega p_c r]_j \quad (4.9)$$

where ω is the rotational speed, and f is the friction coefficient for asperity contact. Since the temperature change is assumed to be linearly dependent on the thermal load, the steady-state temperature at node i is expressed as:

$$T_{si} = \sum_{k=1}^{n} IT_{ik} Q_k \tag{4.10}$$

where Q_K is the steady state heat generation rate per unit area at node k. The temperature influence coefficient IT_{ik} is computed by an off-line finite element analysis. Under transient conditions, using Duhamel's method, the temperature field can be written as

$$T - T_0 = \int_{\tau=0}^{\tau=t} \frac{\partial}{\partial t}[\phi(r,z,\tau,t-\tau)]\mathrm{d}\tau \tag{4.11}$$

where $\phi(r,z,\tau,t-\tau)$ is the Duhamel's auxiliary function, that is the time response of $T - T_0 =$ to a steady heat source, and τ is a dummy temporal variable. ϕ is found empirically from a numerical experiment using a finite element thermal deformation analysis.At time $t = 0+\varepsilon$, the resulting temperature at node i obeys the empirical equation:

$$\frac{T_i - T_{oi}}{T_{si} - T_{oi}} = \frac{\phi_i(\varepsilon, t)}{\sum_{k=1}^{n} IT_{ik}[Q_k(\varepsilon) - Q_k(0)]} \tag{4.12}$$

Where T_i and T_{oi} are the temperature and initial temperature at node i respectively. By plotting the ratio $(T_i - T_{oi})/(T_{si} - T_{oi})$ versus time t, the curve is approximately fitted by $1/(1+a/t)$, where a is a constant. Hence,

$$T_i - T_{oi} = \int_0^t \sum_{k=1}^{n} IT_{ik}[Q_k(\varepsilon) - Q_k(0)] \frac{\partial}{\partial t}\left(\frac{1}{1+\frac{a}{t-\tau}}\right)\mathrm{d}\tau \tag{4.13}$$

Deformation and temperature

There are two types of deformation for a mechanical seal: mechanical and thermal deformation. Mechanical deformation is caused by the pressure in the seal faces and the asperity contact, while the thermal deformation is caused by the viscous and frictional heating. At radial node i, the film thickness is presented as:

$$h_i = h_m + \delta_{mi} + \delta_{ti} \tag{4.14}$$

where h_m is the nominal film thickness, δ_{mi} and δ_{ti} are the mechanical and thermal deformation at radial node i respectively. According to Assumption 3, the mechanical deformation is computed by a quasi-steady influence coefficient approach, that is

$$\delta_{mi} = \sum_{k=1}^{n} IF_{ik} F_k \tag{4.15}$$

where F_k is the total force (pressure force+contact force) on the seal faces at the kth radial node, and IF_{ik} is the influence coefficient that is computed by an off-line finite element analysis. The thermal deformation is more complicated. According to Assumption 3, the thermal deformation can be computed using influence coefficients:

$$\delta_{tsi} = \sum_{k=1}^{n} IQ_{ik} Q_k \tag{4.16}$$

where δ_{tsi} is the steady state thermal deformation at node i. IQ_{ik} is the thermal deformation influence coefficient, which is computed using an off-line finite element analysis. Under transient conditions, using Duhamel's method, and at time $t = 0 + \varepsilon$, the resulting thermal deformation at node i can be computed similarly to the way of computing temperature. Thus for an arbitrary transient,

$$\delta_{ti} - \delta_{toi} = \int_0^t \sum_{k=1}^{n} IQ_{ik} [Q_k(\tau) - Q_k(0)] \frac{\partial}{\partial t} (\frac{1}{1 + \frac{b}{t-\tau}}) \mathrm{d}\tau \tag{4.17}$$

Substituting Equation 4.15, and 4.17 into Equation 4.14, the film thickness at node i is a function of time and other parameters and coefficients. Since the parameters and coefficients can be either measured or computed through finite element analysis, it is possible to predict the trend of the film thickness in the coming future. Meanwhile substituting Equation 4.14 into 4.8, it is possible to predict the leakage rate.

To determine the equilibrium operation of a mechanical seal, numerical iterations are necessary to modify the model, which is shown in Figure 4.7. The first step is to input the physical parameters that are related to the mechanical seal, including the face geometry, loading, material properties, etc. Then based on these inputs, initial guesses for the nominal film thickness h_m, the face temperature T, and film distribution h. The next is to calculate the pressure profile from Reynolds Equation 4.7, the contact force from Equation 4.6, and the face deformation from Equation 4.15 and 4.17, then film thickness can be calculated from Equation 4.14. Afterwards it is necessary to check the convergence of the film thickness h. If the ith iteration equals to the

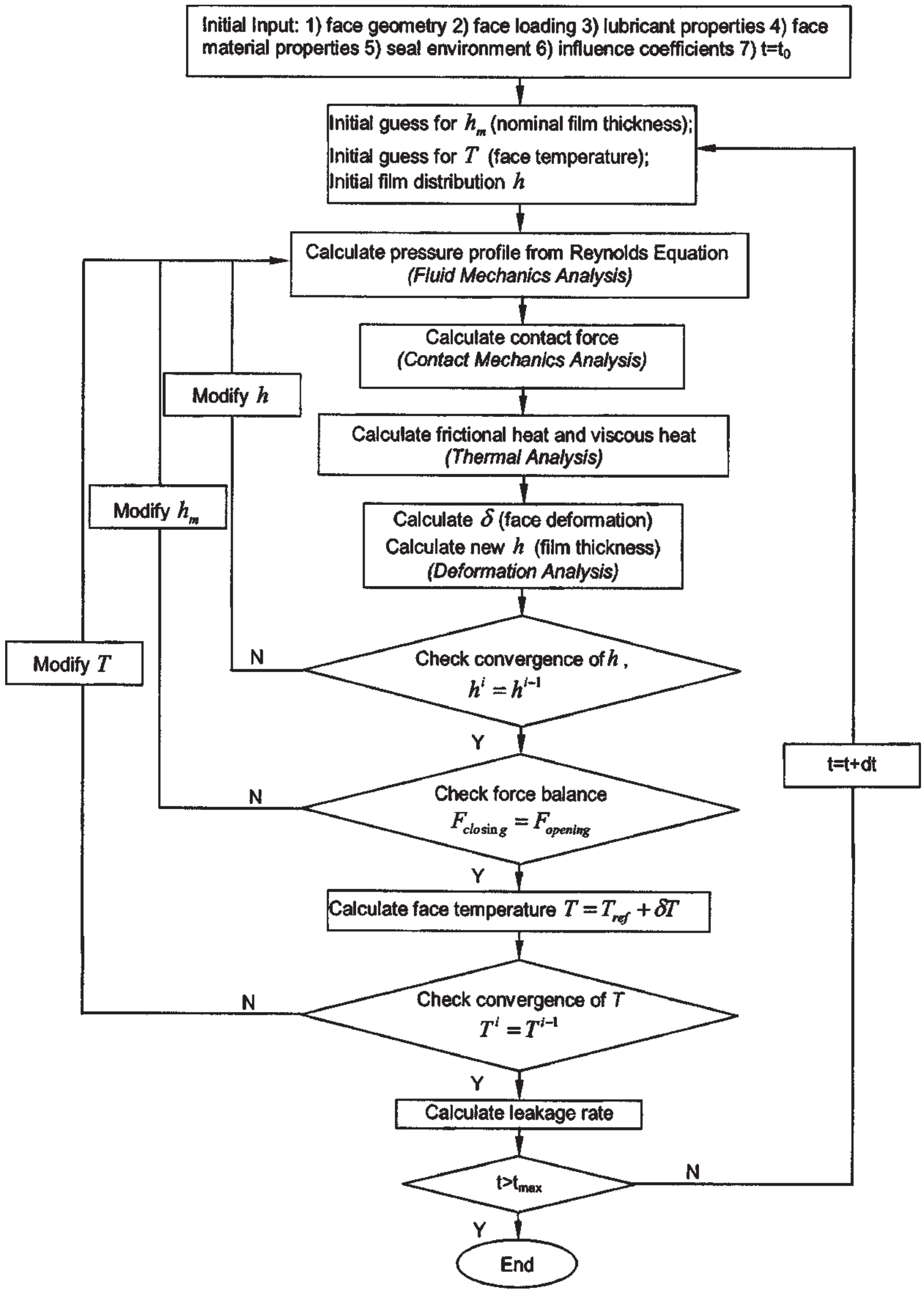

Figure 4.7: Numerical iterations of the physical model (from Salant and Cao (2005))

$(i-1)$th iteration, that is $h^i = h^{i-1}$, then move to the next check, otherwise the value of h has to be modified as

$$h^{i+1} = \lambda h^i + (1-\lambda)h^{i-1} \tag{4.18}$$

where λ is the relaxation factor, with a value of 0.8 or less to achieve convergence (Ruan et al. (1997)). When the film thickness converges, $F_{opening}$ is compared with $F_{closing}$. If the forces are not balanced, the nominal film thickness is modified as

$$h_m^{i+1} = exp[\frac{\Delta f^{i-1} lnh_m^i - \Delta f^i lnh_m^{i-1}}{\Delta f^{i-1} - \Delta f^i}] \tag{4.19}$$

where Δf^{i-1} and Δf^i are the differences between the opening force and the closing force at the ith and $(i-1)$th iterations. After the force balance is achieved, the temperature is calculated from Equation 4.11, then check the temperature convergence. If $T^i \neq T^{i-1}$, the temperature is modified as

$$T^{i+1} = \frac{T^i + T^{i-1}}{2} \tag{4.20}$$

When the temperature converges, the leakage rate can be calculated from Equation 4.8. This procedure is repeated to compute the numerical values at the next time unit. Thus the leakage rate of the mechanical seal can be predicted at any time unit. Then the remaining useful life (RUL) can be predicted as the time from now on until the estimated leakage rate reaches the failure threshold. According to the value of RUL, relevant maintenance decisions can be made, for example, when to prepare for and when to carry out preventive maintenance.

4.3.2 Data-driven model

According to the literature review, it seems that almost all researches about the prognosis of mechanical seals have been taken in physics-based models. The reason might be that on the one hand, the relevant physical knowledge of mechanical seals is already well known. With finite element analysis, it is not difficult to run a physics-based model. On the other hand, it is too expensive to run enough experiments to support the high quantity of data that a data-driven model needs. However, as introduced in Section 4.3.1, the physics-based model is highly dependent on several ideal assumptions, which do not present the real operating conditions. As a result of that, the predicted result of the physics-based model would be biased. Whereas data-driven models can overcome this problem and provide more accurate prediction if enough data is available. Therefore it is still interesting to look into the applicability of data-driven models in the prognosis of mechanical seals.

Proportional Hazard Model (PHM) is a typical data-driven model, which is widely applied in the prognosis of bearings, gearboxes, vibration analysis, etc. Owning to its flexibility and successful applications, it would also be applicable in predicting the hazard rate of mechanical seals.

PHM introduction

Jardine et al. (1999) introduces a Weibull PHM, presented as Equation 4.21, to optimize the condition-based maintenance decisions of vibration monitoring.

$$h(t) = \frac{\beta}{\eta}(\frac{t}{\eta})^{\beta-1} e^{\gamma_1 Z_1(t)+\gamma_2 Z_2(t)+...+\gamma_n Z_n(t)} \tag{4.21}$$

where $h(t)$ is the hazard rate function, and β and η are shape parameter and scale parameter respectively. $Z_1(t), Z_2(t), ..., Z_n(t)$ are time-dependent covariates. And $\gamma_1, \gamma_2, ..., \gamma_n$ are coefficients. The reason why Weibull distribution is selected is that it is flexible to describe various types of machine behaviours. For instance, when $\beta = 1$, it is the same with exponential distribution, which means the hazard rate of the system is independent of time; when $\beta > 1$, the system has increasing hazard rate with time; when $\beta < 1$, the system has decreasing hazard rate with time.

The baseline hazard rate function $h_0(t) = \frac{\beta}{\eta}(\frac{t}{\eta})^{\beta-1}$ is the hazard function of Weibull distributed lifetime, which denotes the contribution to the hazard rate from working age of the machine without influences of covariates. Here β and η can be estimated from event data by regression. If there is no sufficient event data to estimate parameters (e.g. no or only one failure happened in the history), Wang et al. (2000) suggests to use the event data from another identical or similar component or machine with the same manufacture, type and working conditions.

The second part of Equation 4.21 $e^{\gamma_1 Z_1(t)+\gamma_2 Z_2(t)+...+\gamma_n Z_n(t)}$ is the contribution to the hazard rate from condition data, where $Z_1(t), Z_2(t), ..., Z_n(t)$ are features extracted from raw condition data that could indicate the symptoms or the propagations of failure modes. In the case of mechanical seals, these covariates could be the temperature, pressure, speed of the shaft, or the feature values extracted from acoustic emission (AE) signals.

Data collected

In order to run a PHM model, the following data has to be collected:

1. Event data: installation calender time, failure calender time or censoring.

2. Condition data: the raw condition data or the associated covariates that are extracted from original data or both.

3. Censor indicator: to distinguish whether it is a failure data or a censored data.

Here calender time is used to distinguish the working age that is actually used in the model. In practice, right censoring is quite common when collecting data due date. Here right censored data can be simply explained as that when the experiment or inspection is finished, the component does not fail or fails because of other failure modes that are not considered in this experiment or analysis. For censor indicator δ, $\delta = 1$ if failure occurs and $\delta = 0$ if it is right censoring.

The application of PHM in mechanical seals case

By selecting different covariates, PHM can be applied in different ways to estimate the hazard rate function of mechanical seals. Since there are no intrinsic differences between AE technique and vibration monitoring, and they just deal with signals at different frequency ranges. It is possible to apply PHM based on the AE signals, like Lin et al. (2004), in which features extracted from vibration signal, e.g., RFS (standard deviation of the power spectrum of the residual error signal), RTM (mean of the residual error signal), and RTS (standard deviation of the residual error signal), are considered as the covariates in PHM to predict the hazard rate of gearboxes. Similarly, the features extracted from AE signal, such as the essential amplitudes, frequencies, and root mean square(RMS), can be used as the covariates in PHM.

Another option is to use operating parameters as covariates, e.g., the temperature, pressure, operating speed, flow rate, etc. To be simplified, if only three covariates are selected, including temperature $T(t)$, pressure $P(t)$ and operating speed $S(t)$, then the hazard rate function based on PHM is

$$h(t) = \frac{\beta}{\eta}(\frac{t}{\eta})^{\beta-1} e^{\gamma_1 T(t)+\gamma_2 P(t)+\gamma_3 S(t)}$$

The original PHM regards every covariate independent of each other, and no interactions between different covariates are taken into account. However, in the case of mechanical seals, apparently there is interaction between the temperature and pressure and other variates. In order to make the result more accurate, the interactions have to be considered. In this case, the operating speed depends on te design and working requirements, and is relatively independent of temperature and pressure. Hence, only the interaction between temperature and pressure is accounted. The hazard rate function is modified to be

$$h(t) = \frac{\beta}{\eta}(\frac{t}{\eta})^{\beta-1} e^{\gamma_1 T(t)+\gamma_2 P(t)+\gamma_3 S(t)+\gamma_{12} T(t)P(t)} \tag{4.22}$$

Parameter estimation

You et al. (2011) introduces the maximum likelihood estimation (MLE) method to estimate the coefficients and parameters. Firstly, a likelihood function is constructed based on the data collected. When considering right censoring, the right censored data's contribution to likelihood function is $R(t_j)$ that is the survival function, where t_j is the jth ordered time with a dataset Data(j) that includes both event data and condition data. While failure data's contribution to likelihood function is $f(t_j)$ that is the probability density function. Let δ_j denote whether t_j is censored ($\delta_j = 0$) or not ($\delta_j = 1$). Then the general likelihood function taking into right censoring account is

$$L(parameters|data) = \prod_{j:\delta_j=1} f(t_j) \prod_{j:\delta_j=0} R(t_j) \tag{4.23}$$

Since $h(t) = \frac{f(t)}{R(t)}$, substitute $f(t_j) = h(t_j)R(t_j)$ into Equation 4.23, then it is

$$\begin{aligned} L(parameters|data) &= \prod_{j:\delta_j=1} h(t_j)R(t_j) \prod_{j:\delta_j=0} R(t_j) \\ &= \prod_{j:\delta_j=1} h(t_j) \prod_{j} R(t_j) \\ &= \prod_{j} \{[h(t_j)]^{\delta_j} R(t_j)\} \end{aligned}$$

Let $\mathbb{Z}(t) = (T(t), P(t), S(t), T(t)P(t))$ denote the vector of covariates, and $\gamma = (\gamma_1, \gamma_2, \gamma_3, \gamma_{12})$ denotes the vector of coefficients. The likelihood function for this model is Equation 4.24 given m data samples $Data(1, ..., m)$.

$$L(\beta, \eta, \gamma|Data(1, ..., m)) = \prod_{j=1}^{m} \{[h(t_j; \mathbb{Z}(t_j))]^{\delta_j} R(t_j; \mathbb{Z}(t_j))\} \tag{4.24}$$

where

$$R(t_j; \mathbb{Z}(t_j)) = e^{-\int_0^{t_j} h(u; \mathbb{Z}(u)) \mathrm{d}u}$$

Secondly the natural logarithm of Equation 4.24, that is called log likelihood function, is further analysed as it is easier to calculate and still keeps the characters of the likelihood function, which is shown in Equation 4.25.

$$\begin{aligned} l(\beta, \eta, \gamma|Data(1, ..., m)) &= \ln L(\beta, \eta, \gamma|Data(1, ..., m)) \\ &= \sum_{j=1}^{m} \delta_j \ln h(t_j; \mathbb{Z}(t_j)) - \sum_{j=1}^{m} \int_0^{t_j} h(u; \mathbb{Z}(u)) \mathrm{d}u \end{aligned} \tag{4.25}$$

Thirdly, to maximize the likelihood, Equation 4.25 needs to be partial differentiated, and let the partial differentiations equal to 0, for example.

$$\frac{\partial l(\beta, \eta, \gamma|Data(1, ..., m))}{\partial \beta} = 0 \tag{4.26}$$

The same partial differentiation should be taken to η, γ_1, γ_2, γ_3, γ_{12}. Then there would be six different equations to solve six unknown variates, i.e., the estimated $\hat{\beta}$, $\hat{\eta}$, $\hat{\gamma}_1$, $\hat{\gamma}_2$, $\hat{\gamma}_3$, $\hat{\gamma}_{12}$. Hence, there is

$$\hat{h}(t;\mathbb{Z}_{Given}) = \frac{\hat{\beta}}{\hat{\eta}}(\frac{t}{\hat{\eta}})^{\hat{\beta}-1} e^{\hat{\gamma}^T \mathbb{Z}_{Given}} \tag{4.27}$$

which means when given the values of covariates $\mathbb{Z}$, the hazard rate function could be estimated as a function of t. The survival function is then

$$\hat{R}(t;\mathbb{Z}_{Given}) = e^{-\int_0^t h(u;\mathbb{Z}_{Given})\mathrm{d}u} = e^{(\frac{t}{\hat{\eta}})^{\hat{\beta}} e^{\hat{\gamma}^T \mathbb{Z}_{Given}}} \tag{4.28}$$

With the survival function, it is possible to predict the probability that a mechanical seal can survive for a period of time, and the probability that it would fail during a certain period, which also provides information for decision makers about whether it is necessary to maintain or replace the seal. It is also possible to calculate the mean RUL as

$$\begin{aligned} mean\,RUL(t;\mathbb{Z}_{Given}) &= \int_0^\infty R(x|t;\mathbb{Z}_{Given})\mathrm{d}x \\ &= \frac{1}{R(t;\mathbb{Z}_{Given})}\int_t^\infty R(x;\mathbb{Z}_{Given})\mathrm{d}x \end{aligned} \tag{4.29}$$

Randomness of data-driven model

A data-driven model mainly aims to figure out the distribution of a component's lifetime that is a random value. For example, the most common ones are exponential distribution, Weibull distribution, gamma process, Homogeneous Poisson Process (HPP), etc. In the PHM model, it assumes that when there is no influence from external factors, the lifetime of a mechanical seal follows a Weibull distribution, which is the baseline hazard rate function $h_0(t)$. Then by taking into account the covariates, a more realistic hazard rate estimation is given by $h(t)$ in Equation 4.22. The process of identifying the most fitted distribution is usually carried out in a statistical method. For instance, the parameter estimation method, MLE, is a typical statistical methodology.

Due to the randomness of the lifetime, there is no way to calculate a deterministic RUL for a mechanical seal. This is why a PHM model finally computes the mean RUL (Equation 4.29) instead of an exact RUL in the physics-based model. And the estimated result is usually along with a variance or a standard deviation to show the possible fluctuation of the real value. The smaller the variance is, the more accurate the estimation is. Thus it is always pursued to reduce the variance for a data-driven model. In statistics, an effective way to reduce the variance is to increase the sampling size. In the case of PHM, it is important to collect enough event data to improve its precision, since the likelihood function is mainly based on event data.

In comparison with the physics-based model, a data-driven model focuses more on the probability of the occurrence of failures. Therefore, instead of giving a judgement on when a failure would occur, it tries to state the probability that it would fail or survive during a certain period, which usually gives a better support for decision-makers because it takes into account of the stochastic properties. However this is also the reason why it needs a high quantity and quality of data, which is the main limitation of the data-driven models. Another issue is that the estimated data-driven model is constructed based on the history and current data, which might be only accurate enough for short-term prediction. And it needs to be updated regularly when new condition data and event data are collected.

Chapter 5

Twin Screws Wear Monitoring

Since the MPP is mounted upon the wellhead, the whole pump system is subjected to brutal crude oil conditions, e.g., heavy sands, formation water, carbon dioxide and hydrogen sulphide. Therefore corrosion and erosion caused wear is a highlight in the application of MPP. A great many efforts have been taken to research new materials that are high-resistant to corrosion and erosion. According to Klein and Hoffmeister (2008), the components that experience the most serious corrosion and erosion in a MPP are the liner, the shaft nut, the mechanical seals and the screws. The corrosion of the liner is less critical than other three components. The corrosion of the shaft nut and the mechanical seals can be prevented by using high grade corrosion resistant stainless steels. But the wear of the screws is inevitable due to the aggressive medium processed.

Since the screws perform the main function of the pump, the health conditions of the screws determine directly the functioning and capacity of a MPP. Hence, it is very necessary and important to execute condition monitoring (CM) for the screws to predict the coming failure and avoid unnecessary maintenance.

However, for MPP is relatively new technology, most researches about the screws still focus on the design phase, especially the screw geometry. As the most important boosting equipment in subsea field, the CM of the screws in a twin-screw MPP should be a highlight topic sooner or later to improve the availability of the oil production system. Therefore this thesis proposes a new method to monitor and analyse the wear conditions of the screws, including which type of data need to be measured and how to measure, afterwards Hidden Markov Model (HMM) and Hidden Semi-Markov model (HMM) are applied for diagnosis and prognosis, in other words, classifying the wear conditions and predicting the mean remaining useful life (RUL).

5.1 Wear Profile of the Screws

Owing to the special structure of a twin-screw MPP, there are mainly three clearances inside the main pump unit(Vetter et al. (2000b)), as shown in Figure 5.1:

- Circumferential clearance (CC) between the screw peripheral diameter and the liner;
- Radial clearance (RC) between the internal and external diameter of the screw profile;
- Flank clearance (FC) between the flanks of the screw profile

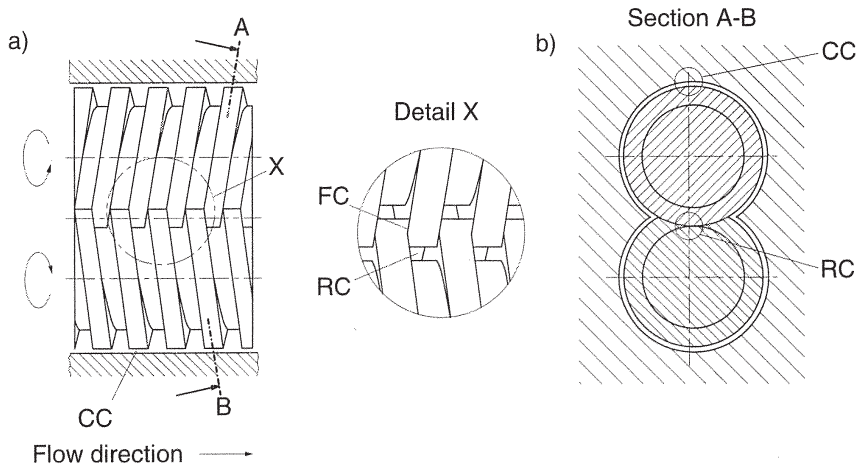

Figure 5.1: Three main clearances inside the pump unit (Vetter et al. (2000b))

In a twin-screw MPP it is unavoidable that a small quantity of pumped flow would go back to the suction area through these clearances, which is called backflow. Usually the amount of the backflow is within the acceptable level due to the high-precision design. However the corrosion and erosion caused wear of the screws can lead to the increase of these three clearances, which results in increasing backflow as well. The more the backflow exists, the less capacity the MPP has. When the wear level reaches a predetermined threshold, the MPP's capacity can no longer meet working requirements, thus corresponding maintenance has to be carried out to replace the screws.

The wear profile of the screws is shown in Figure 5.2. The wear in horizontal direction ($\Delta s_{beginning} -$

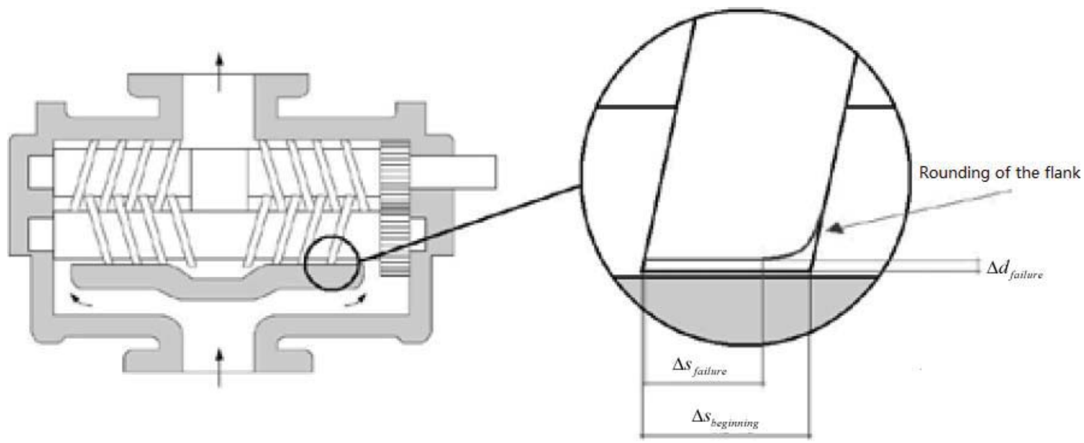

Figure 5.2: The wear profile of the screws (Klein and Hoffmeister (2008))

$\Delta s_{failure}$) leads to increased FC, while the wear in rotation direction ($\Delta d_{failure}$) results in increased RC and CC. $\Delta s_{failure}$ and $\Delta d_{failure}$ are the failure threshold.

5.2 Condition Monitoring and Analysis Method

5.2.1 Data type and measurement

To learn about the wear conditions of the screws, the most direct way seems to measure the $\Delta s_{failure}$ and $\Delta d_{failure}$ shown in Figure 5.2, just like that the wall thickness of pipeline is usually measured to indicate the corrosion conditions of the pipeline offshore. However, unlike the static pipeline, the screws keep rotating all the time with various speed during operation. In addition the precisely designed clearances leave very limited space for sensors. Therefore it is almost impossible to measure them in an on-line condition monitoring system.

Another thinking is that since the wear of screws leads to the increase of backflow, it might be applicable to monitor the backflow to indicate the wear conditions. But the problem is that it is very difficult to obtain the actual amount of backflow. Since the backflow is dynamic in different directions, there is no way to measure the backflow amount directly. In an indirect way, the actual backflow (V_{back}) equals to the theoretical volume flow (V_{theo}) subtracts the actual delivered volume flow (V)(Scharf (2006)), where V_{theo} can be calculated based on the screw geometry, and V can be measured at the pump discharge point. However this is based on the assumption that there is no external leakage through other parts of the pump, such as bearings and seals. Apparently this assumption does not work with a degraded MPP, thus backflow is not a good indicator for the condition monitoring of the screw wear in this case.

Pressure distribution along the screw axis is an important parameter for the performance of a twin-screw MPP, since it reflects the flow distribution and delivery inside the pump. D. Mewes (2008) shows that the backflow determines the shape of the resulting pressure distribution along the screw axis. Hence, the pressure distribution can be measured by installing several pressure sensors along the screw axis to infer the backflow amount, and then indicate the wear conditions.

According to Gao et al. (2011), miniature pressure sensors are applied and mounted in the root grove on the discharge side of the screw, as shown in Figure 5.3. To measure the pressure distribution, it is necessary to mount several pressure sensors uniformly distributed along the screw axis.

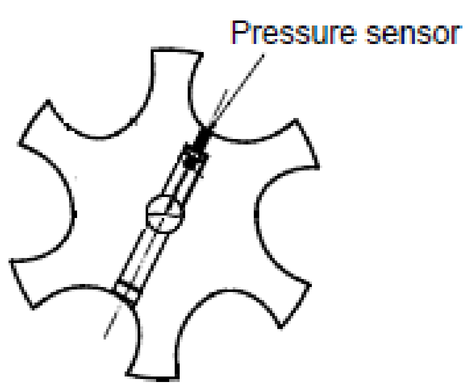

Figure 5.3: The position of the pressure sensor(Gao et al. (2011))

5.2.2 Analysis method

Despite the backflow, other operational parameters, such as GVF, rotation speed of the shaft, differential pressure between the suction and discharge, and fluid viscosity, also have impact on the pressure distribution. Therefore the change of the measured pressure distribution cannot be directly utilized as wear conditional data. To solve this problem, the modelling illustrated in D. Mewes (2008) can be used to calculate the pressure distribution of a healthy twin-screw MPP based on the screw geometry and relevant operational parameters. Then the difference between the measured and calculated pressure distribution can be obtained as $\Delta P = P_{mea} - P_{cal}$. Since P_{cal} indicates the healthy conditions, if ΔP is very small, then the screw is healthy, otherwise it may suffer wear in different degrees. In this way, the influences of the operational parameters are subtracted, and the changing trend of ΔP can reveal the wear trend.

D. Mewes (2008) carries out experiments to verify its modelling for pressure distribution, and the result is shown in Figure 5.4. Seven pressure sensors are mounted equally along the screw axis. It shows that when the modelling takes into account the flank gap (i.e. FC), the calculated values matches the measured ones quite well. Hence, this pressure distribution modelling can be used as a baseline that represents healthy screws. Then a basic estimation could be that the further the measured value deviates from the baseline, the more serious the screw wear is. Thus ΔP is determined as the wear condition indicator.

The next question is to select a mathematical model that uses the datasets of ΔP to identify the current wear condition and further predict the RUL of the screws. Since the real wear condition is unobservable during operation, and ΔP is an indirect indicator, it is easily to think of Hidden Markov Model (HMM). HMM is composed of two stochastic processes, a hidden Markov chain, which is unobservable and represents the real state of the deterioration, and an observable process, which is the observed condition monitoring information from monitoring and tests(Si et al. (2011)). The interconnection between the sequence of unobservable states and the observable process is the essential part of HMM. One advantage of HMM is that it is available for both diagnosis and prognosis. Thus it is applied in this case to classify the wear level and predict the RUL as well. The procedure is shown in Figure 5.5. For the modelling of pressure

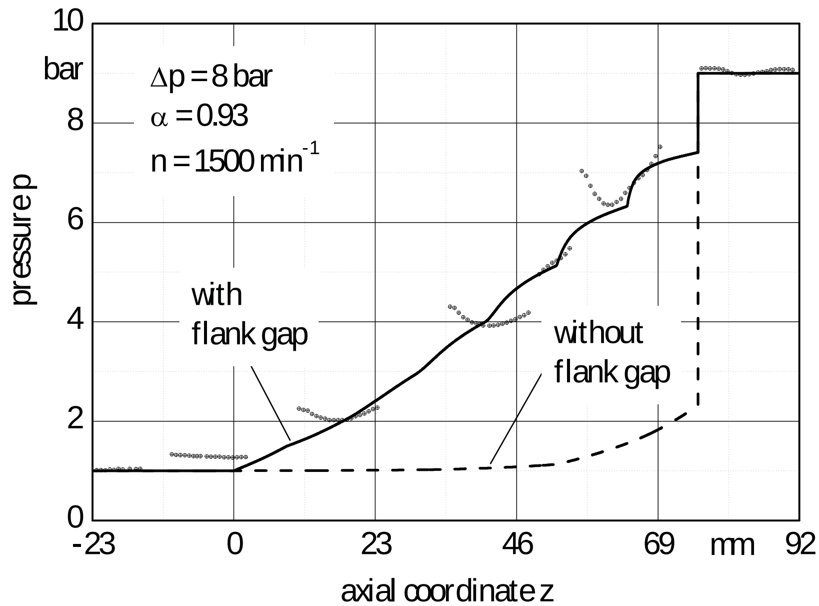

Figure 5.4: Measured (dots) and calculated (continuous line) pressure distribution (D. Mewes (2008))

distribution requires highly the corresponding physics knowledge, which is not the objective of this thesis, it is not explained in detail. More information can be found in D. Mewes (2008). Whereas the theory and application of HMM will be illustrated.

5.3 Hidden Markov Model

5.3.1 Theoretical background

Hidden Markov Model (HMM) is an extension of Markov chain. The Markov chain is a stochastic process which shows how the researched object transits among different states with time. While in a HMM there are two related stochastic processes: a hidden stochastic process that is the real concerned condition states, and another stochastic process which is observable with a sequence of symbols. The hidden stochastic process has the same properties with a Markov chain, i.e., each state has a transition probability distribution that determines which state it will be in the next time unit. And the state selected at time unit t, depends only on the state that was selected at time unit $(t-1)$, thus is independent of the state history from initial time 0 to time unit $(t-2)$.

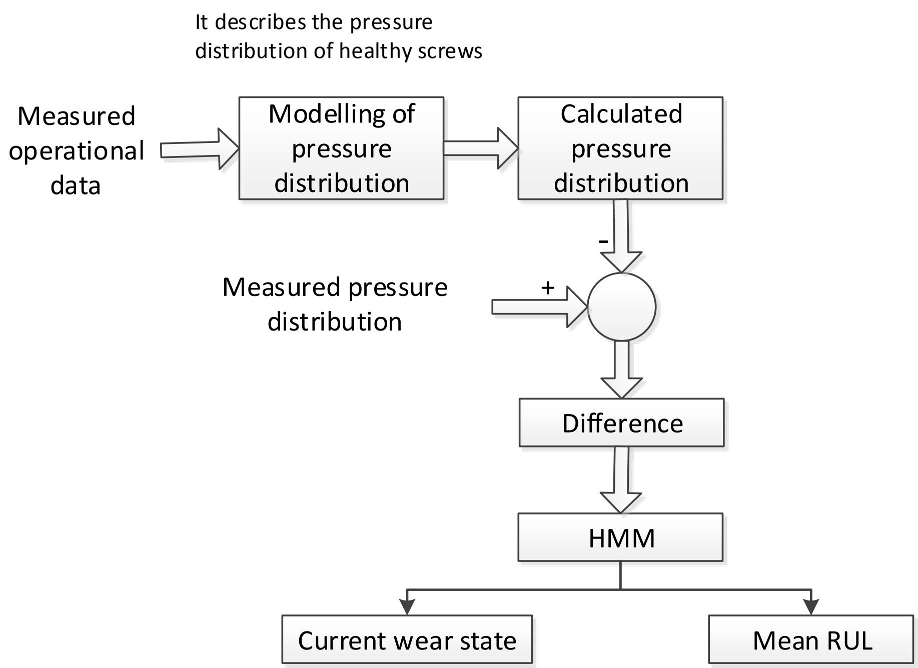

Figure 5.5: Procedure of condition monitoring and analysis of screw wear

According to Qiu et al. (2005), a HMM has the following elements:

1. N, the number of possible (hidden) states, denoted by $\{1, 2, ..., N\}$. The state at time t is s_t. For continuous process, usually it is divided into segments to be discrete states.

2. Transition matrix $\mathbf{A} = \{a_{ij}, 1 \leq i, j \leq N\}$ represents the probability of moving from state i to state j, and $a_{ij} = P(s_{t+1} = j | s_t = i), 1 \leq i, j \leq N$, with $a_{ij} > 0$ and $\sum_{j=1}^{N} a_{ij} = 1$.

3. The observation probability distribution in state i, which is also called emission matrix, denoted by $\mathbf{B} = \{b_i(k)\} = P(O_t = k | s_t = i)$, where k is the observation symbol, and O_t is the observation at time t. These distributions are either mass functions in case of discrete observations or specified using a parametric model (e.g., Gaussian) in the case of continuous observations.

4. The initial state distribution $\pi = \{\pi_i\}$ where $\pi_i = P(s_1 = i), 1 \leq i \leq N$ with $\pi_i \geq 0$ and $\sum_{i=1}^{N} \pi_i = 1$.

Generally a HMM is represented by a triplet $\lambda = (\mathbf{A}, \mathbf{B}, \pi)$. A simple discrete HMM example is shown in Figure 5.6. The three tables in Figure 5.6 represents the emission matrix $\mathbf{B}$, in which the first column is four distinct observations for each state.

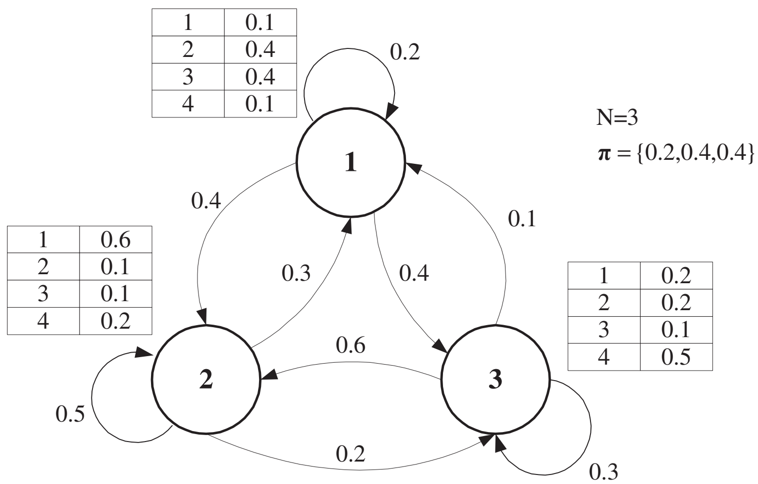

Figure 5.6: A discrete HMM example (Qiu et al. (2005))

There are three basic problems of interest to be solved given a HMM λ:

- Problem 1: given λ and an observation sequence $O = (o_1, o_2, ..., o_T)$, how to compute the probability of the observation sequence, i.e., $P(O|\lambda)$. This is to evaluate how well a given model matches a given observation sequence. Then the model that best fits the observed data can be figured out, which is widely used in fault diagnostic. This probability can be calculated through forward-backward procedure, which is introduced in Baum et al. (1967).

- Problem 2: given λ and an observation sequence $O = (o_1, o_2, ..., o_T)$, how to find the hidden state sequence $S = (s_1, s_2, ..., s_T)$ that has most likely produced the observation sequence, i.e., that maximizes $P(S|O, \lambda)$. This problem is solved by Viterbi algorithm(Viterbi (1967)).

- Problem 3: find the model parameters $(\mathbf{A}, \mathbf{B}, \pi)$ that best fit the observation sequence O, i.e., that maximize the probability $P(O|\lambda)$. It is solved by the Baum-Welch algorithm(Dempster et al. (1977)).

5.3.2 Application of HMM

In the case of screws wear situation, the observed stochastic process is the random values of ΔP in time series, while the hidden stochastic process is the state transition of the real wear procedure. Generally a wear procedure can be divided into four phases according to the wear degrees: normal, slight wear, medium wear, serious wear (or failure). Thus the states space is denoted by $\{1,2,3,4\}$ that represent four different wear degrees.

The value of ΔP consists of two parts: the real deviation caused by the wear of the screws, and noises that include environment noise and uncertainty cased by data measurement. For healthy screws, ΔP equals to the noises that should fluctuate randomly around value zero. While when wear appears, ΔP would be obviously away from zero. To be simplified, the possible values of ΔP can be classified into ascending groups, e.g., 5 groups denoted by $\{1,2,3,4,5\}$, where Group 5 has the highest possible values and Group 1 contains the lowest ones. The estimated result should be more accurate if more groups are classified, but the computing load is also increased.

To investigate the wear conditions of the whole screw, several pressure sensors are required to be mounted along each screw axis. Thus HMMs analysis should be taken at each position of the sensors to identify the local wear conditions. The analysis of each point is identical and independent of each other. After all local wear conditions are identified, the global wear conditions of the whole screw is obtained. Then it is possible to decide whether it is necessary to replace the screw according to the number of local points that have serious wear. The mean RUL of the screw can also be estimated by analysing the mean RUL of each point. The procedure is shown in Figure 5.7, assuming the number of pressure sensors along one screw is m. Since the analysis at each point is identical and independent, the following part of the thesis focuses only on the diagnosis and prognosis based on HMMs at a single point.

5.3.3 Diagnosis based on HMMs

Diagnosis in this case is to identify the current wear state of the screw, which is based on the recognition capacity of HMMs. Firstly, a basic HMM for the wear conditions of the screw is established in Figure 5.8. Since the wear process is irreversible and quite slow with time, it can

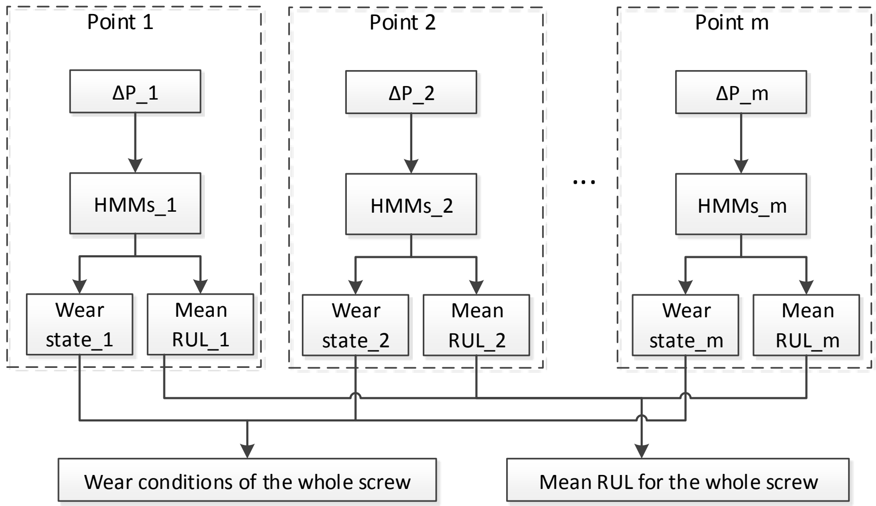

Figure 5.7: The wear conditions identification and prediction for a whole screw

only transit one state to the next one gradually.

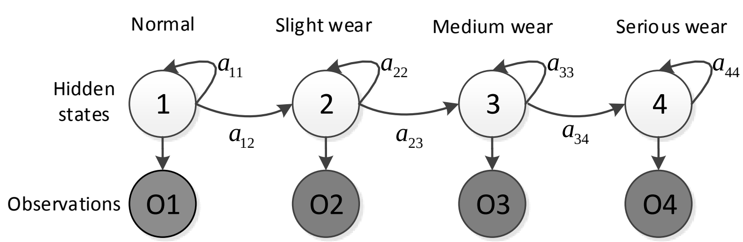

Figure 5.8: A basic HMM for the wear conditions of the screw

To recognize which state the screw is currently in, four HMMs have to be trained for the four states respectively. In detail, four groups of datasets are required from the screw in four different states, which can be obtained either by running four experiments with four screws in different states (i.e., a normal screw, a slight wear one, a medium wear one, and a serious wear one), or getting data for the four life phases from the whole lifetime data of a screw. Then introducing the current observed data, the probability $P(O|\lambda)$ is calculated for each trained model, and the one with the maximum log-likelihood (i.e., $logP(O|\lambda)$) is the current state, which means the current observations are most likely produced from this trained HMM. The schematic demonstration is shown in Figure 5.9.

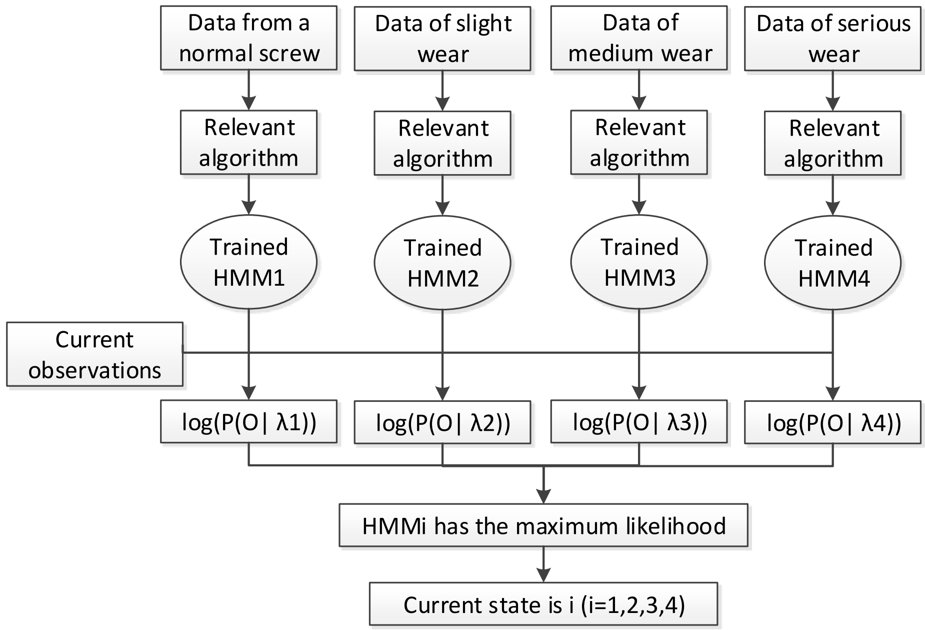

Figure 5.9: Diagnosis procedure based on HMMs

5.3.4 Prognosis

Prognosis in this case is to predict the mean RUL of the screw. A new HMM needs to be trained by the whole lifetime data. Thus the four groups data, that are used to train four different HMMs, now are used together to train a single HMM that represents the transition process of the whole lifetime rather than an individual wear phase, as shown in Figure 5.10.

To estimate the mean RUL, another parameter has to be introduced, which is D_i, the sojourn duration it stays in state i. If the sojourn duration in each state is estimated, then the mean RUL can be predicted. Here two methods are presented to solve this question: straightforward method and Bayesian Model Averaging (BMA) method.

Straightforward method for HMM

Since the model is strictly left-right, the RUL can be estimated as the summation of the residual time of staying in the current state and the duration of staying in the future health states before entering the failure one. In this model the state 4 serious wear is regarded as failure. If the current state is identified as i $(i = 1,2,3)$, let D_i^t denote the residual sojourn time in the state i at

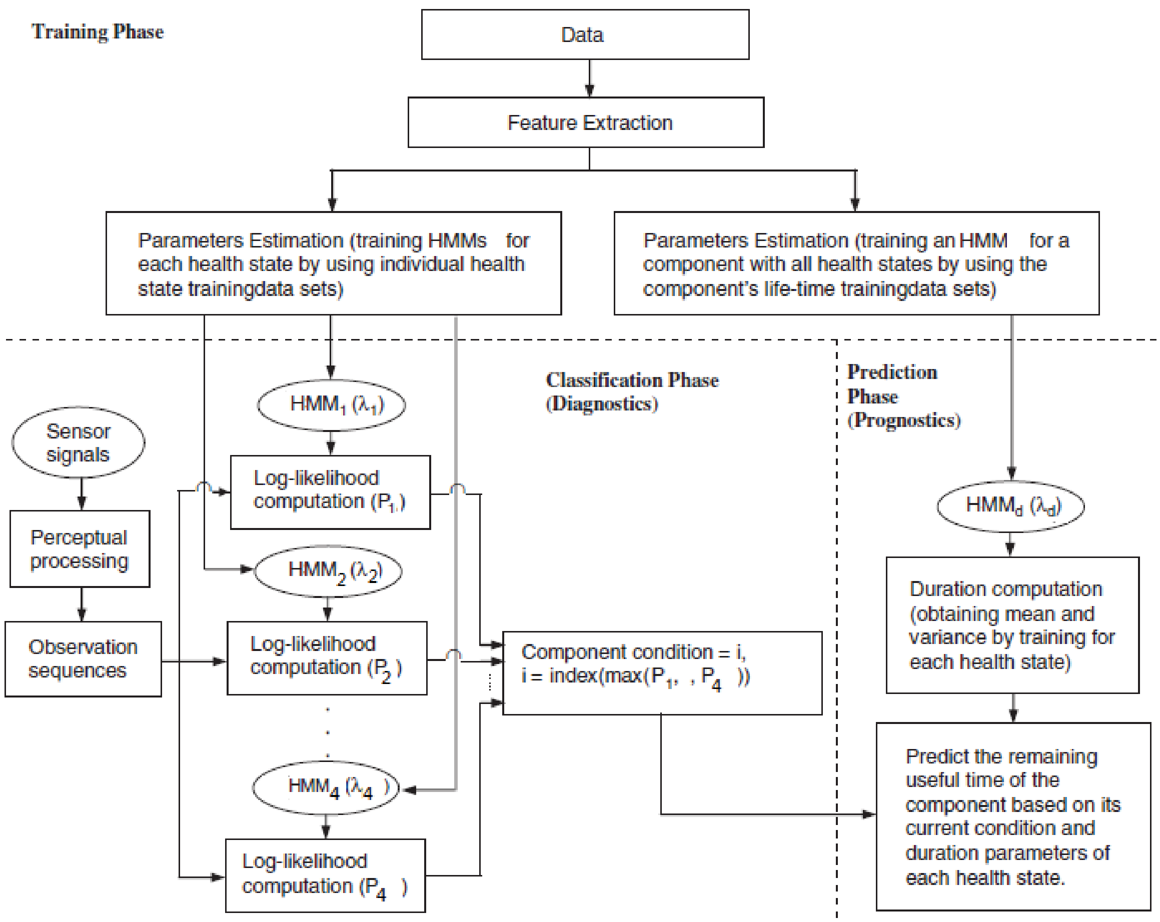

Figure 5.10: Diagnosis and prognosis based on HMMs(adjusted from Dong and He (2007))

the current time t, then the RUL is calculated as Equation 5.1 (Le et al. (2014a)).

$$RUL_i^t = D_i^t + \sum_{j=i+1}^{3} D_j \tag{5.1}$$

The random variable $D_i^t = D_i - D_{ipast}$, where D_{ipast} is the time that it has spent in the state i, which can be estimated through Viterbi algorithm. Viterbi algorithm can find the most likely state sequence given the observations and the HMM λ. Then $\overline{D_i}$ could be obtained by simply counting the time units that it has spent in the state i through the state sequence.

D_i is also a random variable so that its probability mass function is computed rather than an exact value of D_i. Let $P_i(d)$ denote the probability of the event of staying in state i for exactly d time units, which is presented in Equation 5.2 (Dong and He (2007)), where a_{ii} is the element in transition matrix **A** of the HMM0(λ_0) trained by the whole lifetime data sets. This equation means that $P_i(d)$ is the joint probability that it takes the self-loop for $(d-1)$ times and takes the out-going transition once.

$$P_i(d) = a_{ii}^{d-1}(1-a_{ii}) \tag{5.2}$$

Since D_i is independent of each other, the mean RUL_i^t can be computed in Equation 5.3,

$$mean\,RUL_i^t = \overline{D}_i - D_{ipast} + \sum_{j=i+1}^{3} \overline{D}_j \tag{5.3}$$

where $\overline{D}_i$ is the mean sojourn time in state i, and there is

$$\overline{D}_i = \int_0^{\infty} tP_i(t)\mathrm{d}t \tag{5.4}$$

BMA method for HMM

BMA method calculates the RUL distribution as an average of the posterior distributions under each constituent model, weighted by their posterior model probability. The following derivation procedure is based on the theory illustrated in Le et al. (2014b). The probability mass function is given by

$$P(RUL_i^t = n) = P(s_{t+n} = 4, s_{t+n-1} \neq 4, ..., s_{t+1} \neq 4 | s_t = i)$$

Denote $h_i^{(n)} = P(RUL_i^t = n)$. Since the model is strictly left-right topology HMM, at state 3, there is

$$\begin{aligned} h_3^{(1)} &= a_{34} \\ h_3^{(n)} &= a_{33}h_3^{(n-1)} = ... = a_{33}^{(n-1)}a_{34} \end{aligned} \tag{5.5}$$

At state 2, there is

$$\begin{aligned}
h_2^{(1)} &= a_{24} = 0 \\
h_2^{(2)} &= a_{22}h_2^{(1)} + a_{23}h_3^{(1)} = a_{23}a_{34} \\
h_2^{(n)} &= a_{22}h_2^{(n-1)} + a_{23}h_3^{(n-1)} = a_{22}(a_{22}h_2^{(n-2)} + a_{23}h_3^{(n-2)}) + a_{23}h_3^{(n-1)} = \ldots \\
&= a_{22}^{n-2}a_{23}a_{34} + a_{23}\sum_{i=0}^{n-3} a_{22}^{i}a_{33}^{n-i-2}a_{34}
\end{aligned} \tag{5.6}$$

At state 1, there is

$$\begin{aligned}
h_1^{(1)} &= h_1^{(2)} = 0, h_1^{(3)} = a_{12}a_{23}a_{34} \\
h_1^{(n)} &= a_{11}h_1^{(n-1)} + a_{12}h_2^{(n-1)} = \ldots = a_{11}^{n-3}h_1^{(3)} + a_{12}\sum_{i=0}^{n-4} a_{11}^{i}h_2^{(n-i-1)} \\
&= a_{11}^{n-3}a_{12}a_{23}a_{34} + a_{12}\sum_{i=0}^{n-4} a_{11}^{i}[a_{22}^{n-i-3}a_{23}a_{34} + a_{23}\sum_{j=0}^{n-i-1} a_{22}^{j}a_{33}^{n-j-2}a_{34}]
\end{aligned} \tag{5.7}$$

Hence, the RUL distribution at each state is computed. The mean RUL_i^t is

$$meanRUL_i^t = \int_0^{\infty} nP(RUL_i^t = n)\mathrm{d}n \tag{5.8}$$

In comparison, straightforward method is much easier then BMA method, but may be too simple to get an accurate enough result. BMA method takes into account the backward transition probabilities and computes an average of the posterior distributions, thus is more advanced than straightforward. The common point is that both of them are just geometrically decaying functions of d or n, for HMM follows the Markov chain properties. However, it has been widely argued that most real-life applications would not obey this function (Dong and He (2007)). Therefore Hidden Semi-Markov Model (HSMM) is introduced to improve the duration estimation.

5.4 Hidden Semi-Markov Model

In HMM, the inherent Markov property makes the sojourn time in each state geometrical or exponential distributed, which is not often true in practice. HSMM could overcome this problem by allowing arbitrary probability distributions such as Gaussian or Gamma for the state sojourn time (Le et al. (2014a)). In addition to the $\lambda = (\mathbf{A}, \mathbf{B}, \pi)$ for HMM, a HSMM is denoted by $\lambda = (\mathbf{A}, \mathbf{B}, \mathbf{D}, \pi)$, where $\mathbf{D}$ is the matrix of the parameters for the state sojourn time distribution. Assume the state sojourn time is Gaussian distributed, since it is the most commonly used, then $\mathbf{D} = \{(\mu_i, \sigma_i)\}$, where μ_i and σ_i are the mean and standard deviation for D_i.

Dong and He (2007) illustrates the HSMM structure by defining macro-states and micro-states, as shown in Figure 5.11. The macro-states are the same with the hidden states presented in a HMM. It assumes that under each macro-state there are a group of micro-states that show the wear process under the macro-state. Even though the macro-states transition follow the Markov chain properties, the micro-states transition within one macro-state is assumed to be Gaussian distributed instead of Markov chain, that is the reason why the model is called "Semi-Markov".

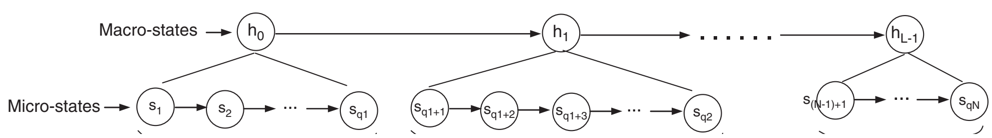

Figure 5.11: HSMM structure(from Dong and He (2007))

The diagnosis and prognosis procedure based on HSMM is the same with HMM, which is shown in Figure 5.10. The main difference is that HSMM calculates RUL based on the Gaussian (or others) distributed D_i, while HMM uses geometrically distributed D_i as demonstrated in Section 5.3.4. The straightforward method and BMA method are also available in the case of HSMM.

Straightforward method for HSMM

Recall the Equation 5.1, where $D_i^t = D_i - D_{ipast}$. Given that D_i is Gaussian distributed, i.e., $D_i \sim N(\mu_i, \sigma_i)$, it can be deduced that the residual time D_i^t follows $N(\mu_i - D_{ipast}, \sigma_i)$ but truncated to the left of zero, since there should be $D_i > D_{ipast}$. Denote $Z = \sum_{j=i+1}^{3} D_j$, then $Z \sim N(\mu_z, \sigma_z)$ where $\mu_z = \sum_{j=i+1}^{3} \mu_j$ and $\sigma_z = \sqrt{\sum_{j=i+1}^{3} \sigma_j^2}$, since D_i is independent of each other. Thus RUL_i^t

becomes the summation of a truncated normal distributed D_i^t and a normal distributed Z. The cumulative distribution function of RUL_i^t is given by (Le et al. (2014a)):

$$P(RUL_i^t \leq x) = F_{RUL}(x) = \frac{1}{1-\Phi(\frac{a}{\sigma})}\int_{-\infty}^{x-a}[\Phi(\frac{x-u}{\sigma})-\Phi(\frac{a}{\sigma})]\phi(u)\mathrm{d}u \tag{5.9}$$

where $a = -\frac{\mu_i - D_{ipast}}{\sigma_z}$, $\sigma = \frac{\sigma_i}{\sigma_z}$, and $\phi(\cdot)$ and $\Phi(\cdot)$ are the probability density function and the cumulative distribution function of the standard normal distribution.

BMA method for HSMM

Like the BMA method for HMM, here it computed RUL also by the following backward recursive equations. The following deducing procedure is based on the theory illustrated in Dong and He (2007). Since the model is strictly left-right structure, at state i, it either stays in i with probability of a_{ii} or transits to the next state $(i+1)$ with the probability of $a_{i,i+1}$. Then at state 3:

$$RUL_3 = D_3 \sim N(\mu_3, \sigma_3) \tag{5.10}$$

At state 2:

$$RUL_2 = a_{22}(D_2 + D_3) + a_{23}D_3 = a_{22}D_2 + (a_{22}+a_{23})D_3$$

Since a_{ij} is constant, with normal distribution properties, there is $a_{22}D_2 \sim N(a_{22}\mu_2, a_{22}\sigma_2)$ and $(a_{22}+a_{23})D_3 \sim N((a_{22}+a_{23})\mu_3, (a_{22}+a_{23})\sigma_3)$, then

$$RUL_2 \sim N(a_{22}\mu_2 + (a_{22}+a_{23})\mu_3, \sqrt{a_{22}^2\sigma_2^2 + (a_{22}+a_{23})^2\sigma_3^2}) \tag{5.11}$$

At state 1:

$$\begin{aligned} RUL_1 &= a_{11}(D_1 + RUL_2) + a_{12}RUL_2 \\ &= a_{11}(D_1 + a_{22}D_2 + (a_{22}+a_{23})D_3) + a_{12}(a_{22}D_2 + (a_{22}+a_{23})D_3) \\ &= a_{11}D_1 + (a_{11}a_{22} + a_{12}a_{22})D_2 + (a_{11}a_{22} + a_{12}a_{22} + a_{11}a_{23} + a_{12}a_{23})D_3 \end{aligned} \tag{5.12}$$

Since RUL_1 is the linear summation of three independent Gaussian distributions, RUL_1 is also normal distributed, and the mean and standard deviation can be calculated in the same way with calculating for RUL_2.

5.5 Numerical Example of HMM

With HMM toolbox in Matlab, it is possible to execute the forward-backward algorithm, Viterbi algorithm, and Baum-Welch algorithm that are needed to train HMMs. Since there are no available data sources from the real practice, this thesis would try to make some datasets to show how HMM can be well applied in the case of screws wear. Thus the numerical results would not provide any practical help, it is only an example that HMM can be utilized for diagnosis and prognosis. The HMM toolbox in Matlab refers to Murphy (2005).

5.5.1 Data generation

There are four hidden states defined, thus four different groups of datasets are necessary to train four HMMs corresponding to the hidden states. Each group of datasets is denoted by a 20×30 matrix, which means the observation sequence length is 30 time units and 20 sets of observation sequence are used to train one HMM. Apparently the more datasets are used, the more accurate the trained result would be. Since this example does not have any practical meaning, to be simplified, only 20 sets of data are used to show how it works.

In state 1, the screws are normal, thus the obtained difference between the measured and theoretically calculated pressure should be only noises caused by measurement. It is very common to represent the noises by Gaussian distribution with mean of 0 and standard deviation of 1, i.e., $N(0,1)$. Therefore, for Group 1 of datasets, the code ">> *datasets1=randn(20,30)*" in Matlab is used to generate a 20×30 matrix that is randomly Gaussian distributed.

In state 2, in additions to the measurement noises, the slight wear of the screws would lead to the further deviation from the theoretically calculated pressure. Hence, *datasets2* for the state 2 is defined as

$$datasets2 = random\ values\ from\ N(0,1) + e^{0.2t+0.5}$$

The part ($e^{0.2t+0.5}$) could be any other distribution that can make *datasets2* different from *datasets1*. Since *datasets2* should also be a 20 × 30 matrix, the value range of t is discrete values {0.01, 0.02, 0.03, ..., 6}. In the same way, in state 3, there is

$$datasets3 = random\ values\ from\ N(0,1) + e^{0.5t+1}$$

and in state 4, there is

$$datasets4 = random\ values\ from\ N(0,1) + e^{0.8t+1.2}$$

For simplification, it is reasonable to classify the values in each group of datasets into several levels to transform the original data into finite and discrete observations. For instance, the data is classified into 8 levels in this example, where Level 1 means the smallest values, and Level 8 means the largest ones. In this way, the observations become simple $\{1,2,3,4,5,6,7,8\}$ instead of the original data directly from the Gaussian distribution or others.

5.5.2 Simulation results

With four hidden states and eight possible observations, the estimated parameters of the trained HMM1, HMM2, HMM3, HMM4 are shown below. The log-likelihood for each HMM is so small because the datasets used for training is too less, only 20 sets. For state 1, the corresponding HMM1 is $\lambda_1 = (\pi, \mathbf{A}, \mathbf{B})$. In detail, $\pi_1 = 0.4597$ means the probability that the initial state is 1 is 0.4597, $a_{12} = 0.4186$ means the probability that it would transit from state 1 to state 2 is 0.4186, and $b_{13} = 0.0005$ means the probability that the observation is 3 when it is in state 1 is 0.0005. After the HMMs are well trained, it is possible to do diagnosis when the current observations are obtained. To verify the HMMs are able to identify the current state, one dataset is extracted from each group of data as current observations. Then the log-likelihood (i.e., $logP(newdata|\lambda)$) is calculated for each HMM, and the one with the maximum log-likelihood is the current state. The analysis results are shown below, where $-Inf$ means negative infinity.

The results show a strong recognition ability of HMM. When the new data comes from Group 1, HMM1 has the maximum log-likelihood, and when the new data comes from Group 2, HMM2

```
HMM1 - State1
loglikelihood1 = -432.6558

π1  =    (0.4597    0.0338   0.0073 0.4992)

A1  =     0.1139    0.4186    0.3311    0.1363
          0.4529    0.1621    0.0109    0.3741
          0.2754    0.1854    0.1840    0.3551
          0.1651    0.2490    0.1227    0.4632

B1        0.4450    0.5545    0.0005         0         0         0         0         0
          0.5200    0.4744    0.0056         0         0         0         0         0
          0.6770    0.3083    0.0147         0         0         0         0         0
          0.4434    0.5529    0.0036         0         0         0         0         0
```

```
HMM2 - State2
loglikelihood2 = -369.4103

π2  =    (0.5046    0.1855   0.0898   0.2201

A2        0.8935    0.0093    0.0924    0.0047
          0.0060    0.7958    0.0085    0.1897
          0.7528    0.0697    0.1244    0.0531
          0.0173    0.6194    0.0261    0.3371

B2        0     0.0000    0.2142    0.7827    0.0031         0         0         0
          0     0.0673    0.8185    0.1142    0.0000         0         0         0
          0     0.0000    0.0426    0.9184    0.0390         0         0         0
          0     0.0000    0.3320    0.6634    0.0046         0         0         0
```

```
HMM3 - State3
loglikelihood3 = -480.1558

π3  =    (0.2081    0.1253     0.45 0.2167)

A3  =     0.5571    0.3430    0.0000    0.0999
          0.6753    0.2482    0.0000    0.0764
          0.0000    0.0000    1.0000    0.0000
          0.8507    0.0286    0.0000    0.1208

B3  =     0     0.0000    0.0000    0.0010    0.3741    0.6248         0         0
          0     0.0000    0.0000    0.0002    0.4179    0.5818         0         0
          0     0.0185    0.4444    0.5037    0.0333    0.0000         0         0
          0     0.0000    0.0000    0.0221    0.3014    0.6765         0         0
```

```
HMM4 - State4
loglikelihood4 = -729.1106

π4  =    (0.4162    0.2109    0.2684 0.1046)

A4  =     0.7473    0.0881    0.0008    0.1637
          0.3270    0.2202    0.1101    0.3427
          0.0042    0.0220    0.9158    0.0580
          0.6442    0.0786    0.1324    0.1447

B4  =     0     0.0025    0.0969    0.1365    0.2732    0.3452    0.1457    0.0000
          0     0.0001    0.1542    0.3027    0.0230    0.2896    0.1900    0.0404
          0     0.0007    0.0130    0.0719    0.0000    0.0065    0.0081    0.8998
          0     0.0019    0.1045    0.3125    0.0738    0.2921    0.1568    0.0583
```

log-likelihood	HMM1	HMM2	HMM3	HMM4
data_new1	-20.8139	-Inf	-Inf	-Inf
data_new2	-Inf	-21.9356	-22.3728	-56.2245
data_new3	-Inf	-Inf	-19.3988	-38.2095
data_new4	-Inf	-Inf	-Inf	-19.3757

has the maximum log-likelihood, etc.

5.5.3 Mean RUL estimation

To estimate the mean RUL, another HMM needs to be trained by the whole lifetime data. With the four groups of datasets together, the estimated parameters of the trained HMM0 is shown below. According to Equation 5.1 and 5.3, and the values of **A**0, the mean sojourn time in each state can be calculated, and the results are shown in Table 5.1. In state 1, the mean sojourn time is 1000 time units. In state 4, that is the failure state, the sojourn time is infinite, which means that if no maintenance activities are carried out, it will always stay in the failure state once it jumps into it.

Table 5.1: Estimated mean duration in each state

State	1	2	3	4
Mean duration	1000	285.7	39.83	Inf

To calculate the residual sojourn time in state i at current time t, the function of "*hmmviterbi*"

```
HMM0 - whole lifetime
loglikelihood0 = -2716

π0 =  (0.1888    0.4159    0.2573 0.138)

A0 =   0.9990    0.0000    0.0004    0.0006
       0.0000    0.9965    0.0010    0.0025
       0.0005    0.0029    0.9749    0.0217
       0.0002    0.0008    0.1947    0.8042

B0 =   0.1171    0.8039    0.0790    0.0000    0.0000    0.0000    0.0000    0.0000
       0.0000    0.0000    0.0176    0.3940    0.2346    0.3539    0.0000    0.0000
       0.0000    0.0416    0.5165    0.1993    0.0000    0.0000    0.0657    0.1769
       0.0000    0.0446    0.6002    0.1119    0.0000    0.0000    0.0665    0.1768
```

in Matlab is utilized to estimate the most likely states sequence based on the history observations. For instance, the current time is 800 time units, and the last 800 observations at each time unit have been recorded, then the most likely states sequence during the past 800 time units can be computed by Viterbi algorithm in Matlab. The result is shown in Figure 5.12. It looks a little unusual that it jumps from state 1 directly to state 3, afterwards it jumps to state 2, which is violate to the strictly left-right model structure that has been established. Looking into the values in the matrix **A**0, it also does not follow a strict left-right model structure. For instance $a_{12} = 0$ that means it is not possible to transit from state 1 to state 2; and $a_{32} = 0.0029$ that means it is possible to transit from state 3 back to state 2, which is obviously against the real situation. However from the view of statistics, there might be two reasons for this problem: the first one is that the datasets are roughly made without deep considerations, which is not so appropriate for the case of screws wear situation; the second reason is the number of datasets are not enough, which leads to the inaccuracy of the estimated parameters in each trained HMM.

According to the computed result, the current state is 2 at the 800th time unit, and the computed states sequence in Matlab shows that it jumps into state 2 at the 628th time unit, which means it has been in state 2 for 800-628=172 time units. Then the mean RUL at the current time is 285.7-172+39.83=153.53 time units.

Even though the datasets made in this example do not fit well the real wear situations of the twin screws, the application of the HMM toolbox in Matlab and the corresponding numerical computation show apparently that HMM do have the potential to carry out the diagnosis and

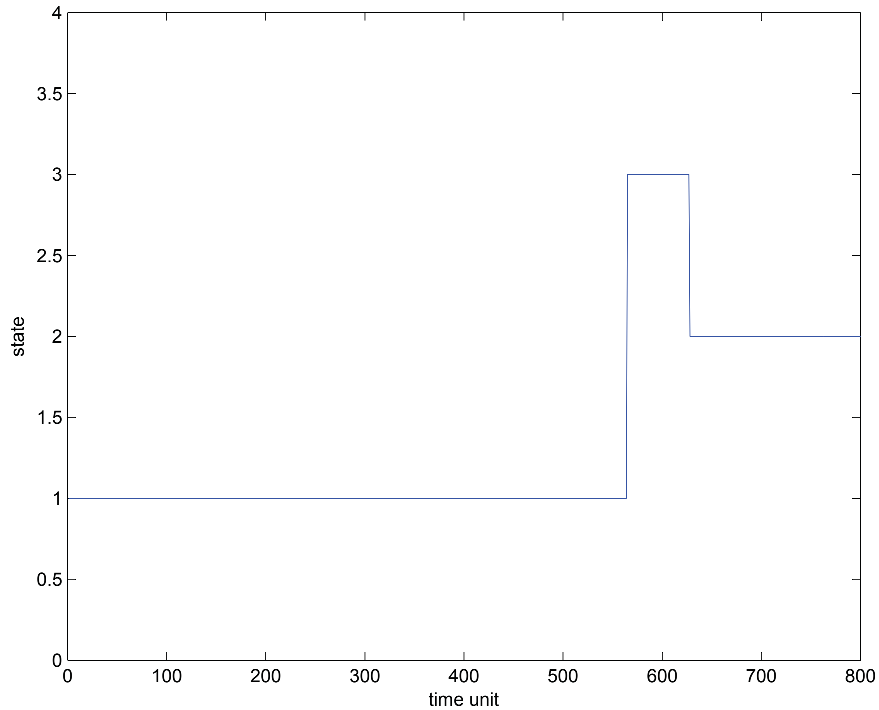

Figure 5.12: The most likely states sequence during 800 time units by Viterbi algorithm in Matlab

prognosis for the wear of the screws. Once real data can be obtained, this model can be applied to identify the current wear conditions and predict the mean RUL. The codes for running this example are provided in Appendix C.

Chapter 6

Summary

6.1 Summary and Conclusions

Even though condition monitoring (CM) techniques have been well developed in other areas such as railway and aerospace, in subsea field it is still in the beginning phase. Mostly the subsea CM focuses on the flow process, e.g., the monitoring of the pressure, temperature, flow rate at the key points, and the detection of oil leakage. But gradually the CM of subsea equipment has been paid more attention. Unlike many literatures present only an abstract framework of CM, this thesis uses the CM of the twin-screw multiphase pump as a case study to show how CM techniques can be applied for the subsea equipment. Through the case study, the following conclusions are made:

1. According to the FMECA of the twin-screw multiphase pump, the critical components are identified as gearbox, twin screws, bearing, mechanical seals, control unit and valves, among which the mechanical seal and twin screws are determined as study objects.

2. For the mechanical seal, the most important feature to show its performance is the film thickness between the rotor and the stator of the mechanical seal. Too thin film thickness would cause the contact of the rotating and the static faces, which is the main reason for the wear of the mechanical seal. Whereas too thick film thickness would lead to oil leakage.

3. There are four existing methods for the CM of a mechanical seal. Thermal method uses

temperature sensors to measure the temperatures of the seal faces. Rotor displacement method uses eddy-current sensors to measure the axial and radial displacements of the rotor. Acoustic emission method uses piezoelectric sensors to detect the acoustic emission from the mechanical seal. Ultrasonic method uses also piezoelectric sensors to measure the reflected ultrasound from the seal faces.

4. A physics-based model can be used to compute the trend of the film thickness with time, which can indicate the occurrence of the contact or leakage, and further predict the remaining useful life (RUL). The proportional hazard model (PHM) can also be applied to estimate the hazard rate function of time for the mechanical seal, and predict the mean RUL.

5. The twin screws are always rotating at various speed during operation, and the shape of the screws is special, therefore it is very difficult to measure the wear conditions directly. An indirect method is to measure the pressure along the screws. The wear of twin screws will lead to the increase of the backflow, which is the flow goes from the discharge area back to the suction area, thus reducing the capacity of the pump. Meanwhile the amount of backflow can influence the pressure distribution along the screws. Hence, the pressure can be measured to analyse the wear conditions of the screws. But the pressure distribution along the screws is also influenced by other operational parameters, e.g., rotating speed, gas void fraction (GVF), flow rate, and viscosity of the flow. To exclude the influences of other operational parameters, firstly based on the physical equations, the theoretical pressure distribution is calculated as a function of these operational parameters for healthy screws. Then the difference value between the measured pressure and the calculated pressure can be utilized as an indicator for the wear conditions of the screws.

6. The difference value between the measured and calculated pressures is further analysed by Hidden Markov Model (HMM). With an numerical example, the HMM is proved to be able to identify the current wear state of the screws and predict the remaining useful life.

6.2 Discussion

This thesis presents the application of condition monitoring (CM) techniques at component level. It would be more interesting to research how to construct a CM system for the whole system to evaluate and predict the conditions of the whole system rather than individual components. The outputs from the CM analysis of components can be the inputs for the system-level CM. Then with some certain algorithms, the condition of the whole system can be estimated based on the condition of each component. A simple solution is Technical Condition Index (TCI) that has been mentioned in Section 2.2, in which the system TCI is computed as the average of each weighted TCI of every component or sub-system. For complex system, more advanced algorithm is necessary to be developed. And it would be better to take into account the impacts of maintenance planning and company strategies.

6.3 Recommendations for Future Work

Usually FMECA is carried out by a team with both professional knowledge and practical experiences. Hence, for practical application, a more professional FMECA worksheet for the twin-screw multiphase pump (MPP) should be implemented.

For the CM of MPP, it is also necessary to research the CM of other critical components including the gearbox, bearings, control unit and valves. Afterwards it is valuable to research the method for estimating the condition of the whole system based on the CM of each critical component.

For mechanical seals, the current analysis methods are mostly physics-based models. This thesis proposed the proportional hazard model (PHM) as a data-driven model to compute the performance of the mechanical seal. But no real data is available to verify this model. If there is real data, it would be very interesting to calculate the numerical results for both physics-based model and data-driven model. Then compare the results of these two types of models to analyse which one is better for the case of mechanical seals, and research whether it is possible to combine the two models together to obtain more comprehensive diagnosis and prognosis for the conditions of the mechanical seal.

For the wear of the twin screws, if more knowledge of the operating process of the screws is acquired, it might be possible to use other parameters as the indicators of the wear of the screws, thus more robust CM of the twin screws can be executed. Besides, Hidden Semi-Markov Model (HSMM) is more advanced than Hidden Markov Model (HMM), since the former assumes the sojourn duration in each state follows arbitrary probability distributions such as Gaussian distribution, which comforts better with the real situation. If real datasets are available, both HMM and HSMM can be trained and compared to show which one is more accurate for diagnosis and prognosis.

Appendix A

Acronyms

MPP Multiphase Pump

CM Condition Monitoring

PM Preventive Maintenance

FMECA Failure modes, effects, and criticality analysis

GVF Gas Void Fraction

GLCC Gas Liquid Cylindrical Cyclone

RPN Priority Number

FFT Fast Fourier Transform

AE Acoustic Emission

PHM Proportional Hazard Model

RUL Remaining Useful Life

HMM Hidden Markov Model

HSMM Hidden Sime-Markov Model

Appendix B

FMECA of A Twin-screw Multiphase Pump

Description of unit			Description of failure			Effect of failure		Failure rate	Severity ranking	RPN
Item	Function	Operational mode	Failure mode	Failure cause or mechanism	Detection of failure	On the subsystem	On the system function			
Two-screw pump										
Gearbox	Power transmission	Running	Breakdown	Structure broken	3	No power transmitted	System stops	2	5	30
			Abnormal vibration	Gear wear; shaft crack; structure deformation; lack of lubrication	2	Gearbox degradation	Reduced efficiency	2	3	12
			Overheating	Lack of lubrication	1	Gearbox degradation	Reduced efficiency	2	2	4
Bearing	Reduce rotational friction and support radial and axial loads	Running	External leakage	Wear	4	Leakage of lubricating oil	Loss of lubricating oil	3	1	12
			Structural deficiency	Misalignment	2	Mechanical degradation	Less output power	3	2	12
			Spurious stop	-	2	Bearing degradation	Less output power	2	3	12
			Breakdown		3	Mechanical damage	May cause system down	2	5	30
			Noise and vibration	Wear; foreign objects	2	Bearing degradation	Reduced lifetime	3	3	18
Mechanical seals	Seal the connection between the shaft and the housing	Sealing	Breakdown	Shock; unbalanced stress; serious wear	3	Cannot seal	Loss control of pressure, may cause pump stops	2	5	30
			Leakage	Large clearance between seal faces	2	Leakage	Reduce the capacity of pump	4	4	32
			Structural deficiency	Wear	2	Leakage	Mechanical degradation	3	2	12

Lubrication	Lubricating and cooling	Running	Lack of oil	No supplementary oil in time	2	Overheat and more friction in gearbox	Reduced efficiency	2	2	8
			Metamorphic of oil	Overused oil	2	Not enough lubrication in gearbox	Degradation of gearbox	2	2	8
Coupling to driver	Coupling	Running	Structural deficiency	Wear	2	Reduced power input	reduced power output	2	3	12
Coupling to driven unit	Coupling	Running	Structural deficiency	Wear	2	reduced power output	Reduced efficiency	3	3	18
Screws	Pumping	Running	Broken	Serious crack; cut	3	Cannot pump	Whole system down	1	5	15
			Corrosion	Chemical reaction	4	Degradation of screws	Reduced output	3	3	36
			Erosion	Physical damage	4	Degradation of screws	Reduced output	2	3	24
			Overheating	Lack of liquid	1	Degradation of screws	Reduced output	2	3	6
Shaft	Power transmission	Running	Noise and vibration	Wear	1	Degradation	Reduced lifetime	3	2	6
			Deformatio	Unbalanced strain	3	Degradation	Reduced output	2	3	18
			Crack	Stress	2	Degradation	With crack increasing, it may cause system down	3	4	24
GLCC (Gas Liquid Cylindrical Cyclone)										
Cyclonic column	Separate gas and liquid	Storing	Corrosion	Chemical reaction	4	Reduced thickness	Reduced lifetime	3	1	12
			Erosion	Physical damage	4	Reduced thickness	Reduced lifetime	2	1	8
Recombination column	Recombine gas and liquid	Storing	Corrosion	Chemical reaction	4	Reduced thickness	Reduced lifetime	3	1	12
			Erosion	Physical damage	4	Reduced thickness	Reduced lifetime	2	1	8
Recirculation										

Port	Liquid input	-	Blockage	Accumulation of particles	2	Less liquid recirculated	Lack of liquid when needed	4	1	8
Line	Transmit recirculated liquid		Leakage	Wear; Looseness	2	Less liquid recirculated	Lack of liquid when needed	3	1	6
Chock valve	Control the recirculated liquid	Open	Delayed operation	Wear; erosion; corrosion	4	Delayed control of liquid	Reduced efficiency	3	2	24
			External leakage	Wear; Seal fails; erosion; corrosion	2	Loss of recirculated liquid	Loss pressure in the line	3	2	12
			Leakage in closed position	Wear; Seal fails; erosion; corrosion	1	No serious influence	No serious influence	3	1	3
			Internal leakage	Wear; Seal fails; erosion; corrosion	2	No serious influence	No serious influence	3	2	12
			Fail to regulate	Wear; erosion; corrosion	1	Cannot control the recirculated liquid	More energy consumed; Not enough recirculated liquid	3	3	9
Slug distributor										
Tangible inlet	Initiate vortex	-	Degradation	Erosion; corrosion	2	Inefficient gas and liquid separation	Reduced efficiency	2	2	8
Standpipe	Gas pass	-	Corrosion	Chemical reaction	4	Reduced thickness	Reduced lifetime of slug distributor	3	1	12
			Erosion	Physical damage	4	Reduced thickness	Reduced lifetime of slug distributor	2	1	8

Tubes	Gas pass	–	Corrosion	Chemical reaction	4	Reduced thickness	Reduced lifetime of slug distributor	3	1	12
			Erosion	Physical damage	4	Reduced thickness	Reduced lifetime of slug distributor	2	1	8
Perforated plate	Liquid pass; stop big particulates	–	Blockage	Accumulation of particles	2	Less liquid pass	Reduced output	4	1	8
Metering holes	Liquid pass; stop big particulates	–	Blockage	Accumulation of particles	2	Less liquid pass	Reduced output	4	1	8
Control										
Control unit	Control of the whole system	Running	Abnormal instrument reading	Disorder	1	Wrong indication	Loss of data of the system	3	2	6
			Erratic output	Abnormal logic	1	Send wrong signal	Disturb the system	3	3	9
			Fail to start on demand	Electrical failure	2	Fail to send signal	Lose control	3	5	30
Wiring	Transmit electrical power and signal	Running	Loose connection	Loose bolt	1	Fail to send signal or power	No corresponding performance when needed	2	3	6
			Electric leakage	Wear	3	Unstable signal	Wrong data inspected; reduced efficiency	2	3	18
Inlet valve	Crude oil inlet	Open	Fail to close on demand	Wear; erosion; corrosion	2	Cannot stop input flow	Disorder of system	3	4	24

			Fail to open on demand	Wear; erosion; corrosion	3	Crude oil goes into the pump	Seriously reduced efficiency	2	5	30
			Delayed operation	Wear; erosion; corrosion	4	Takes longer time to open and close	Reduced efficiency	2	3	24
			External leakage	Wear; erosion; corrosion	3	Less input	Loss of pressure and oil	3	2	18
			Leakage in closed position	Wear; erosion; corrosion	3	Loss pressure	Reduced efficiency	2	2	12
Outlet valve	Flow outlet	Open	Fail to close on demand	Wear; erosion; corrosion	2	Cannot stop output flow	No serious influence	3	1	6
			Fail to open on demand	Wear; erosion; corrosion	3	Crude oil goes into the pump	No output	2	5	30
			Delayed operation	Wear; erosion; corrosion	4	Takes longer time to open and close	No serious influence	2	1	8
			External leakage	Wear; erosion; corrosion	3	Less output	Loss of pressure and oil	3	2	18
			Leakage in closed position	Wear; erosion; corrosion	3	Loss oil	Loss oil	2	2	12
Bypass valve	Let crude oil bypass multiphase pump when pump stops	Close	Fail to open on demand	Wear; erosion; corrosion	3	Crude oil goes into the pump	No output	2	5	30
			Fail to close on demand	Wear; erosion; corrosion	2	No inlet flow to pump	Pump stops	3	4	24

			Delayed operation	Wear; erosion; corrosion	4	Takes longer time to open and close	Slightly reduced efficiency	2	2	16
			External leakage	Wear; erosion; corrosion	3	Less output	Loss of pressure and oil	3	2	18
			Leakage in closed position	Wear; erosion; corrosion	3	Loss oil	Loss oil	2	2	12
Miscellaneous										
Inlet pipe	Transmit inlet flow	-	Corrosion	Chemical reaction	3	Reduced thickness	Reduced lifetime of pipe	3	2	18
			Erosion	Physical damage	3	Reduced thickness	Reduced lifetime of pipe	2	2	12
Outlet pipe	Transmit outlet flow	-	Corrosion	Chemical reaction	3	Reduced thickness	Reduced lifetime of pipe	3	2	18
			Erosion	Physical damage	3	Reduced thickness	Reduced lifetime of pipe	2	2	12
Check valve	Prevent the flow from returning	One direction pass	Leakage	Wear; erosion; corrosion	2	Few flow returns	Less output	3	3	18
Intercooler	Cool the recirculated liquid	Running	External leakage	Seal fails	3	Loss of recirculated liquid	Lack of liquid when needed	2	2	12
			Structural deficiency	Degradation	2	Inefficient cooling	Overheated liquid	3	2	12
Support	Support the equipment	-	Vibration	Loose bolt; wear	1	Unstable support	Unstable of the equipment	4	3	12

Appendix C

Codes for Calling HMM Toolbox in Matlab

```
%Define the number of states and observations for each HMM;
O_1 = 8;
Q_1 = 4;
O_2 = 8;
Q_2 = 4;
O_3= 8;
Q_3 = 4;
O_4 = 8;
Q_4 = 4;

% training data
% the training data is defined in another file

% initial guess of parameters
prior_11 = normalise(rand(Q_1,1));
transmat_11 = mk_stochastic(rand(Q_1,Q_1));
obsmat_11 = mk_stochastic(rand(Q_1,O_1));

prior_21 = normalise(rand(Q_2,1));
transmat_21 = mk_stochastic(rand(Q_2,Q_2));
obsmat_21 = mk_stochastic(rand(Q_2,O_2));

prior_31 = normalise(rand(Q_3,1));
transmat_31 = mk_stochastic(rand(Q_3,Q_3));
obsmat_31 = mk_stochastic(rand(Q_3,O_3));

prior_41 = normalise(rand(Q_4,1));
transmat_41 = mk_stochastic(rand(Q_4,Q_4));
obsmat_41 = mk_stochastic(rand(Q_4,O_4));

% improve guess of parameters using EM
[LL_1, prior_12, transmat_12, obsmat_12] = dhmm_em(data_1, prior_11,
transmat_11, obsmat_11, size(data_1,1));
```

```
LL_1
prior_12
transmat_12
obsmat_12

[LL_2, prior_22, transmat_22, obsmat_22] = dhmm_em(data_2, prior_21,
transmat_21, obsmat_21, size(data_2,1));
LL_2
prior_22
transmat_22
obsmat_22

[LL_3, prior_32, transmat_32, obsmat_32] = dhmm_em(data_3, prior_31,
transmat_31, obsmat_31, size(data_3,1));
LL_3
prior_32
transmat_32
obsmat_32

[LL_4, prior_42, transmat_42, obsmat_42] = dhmm_em(data_4, prior_41,
transmat_41, obsmat_41, size(data_4,1));
LL_4
prior_42
transmat_42
obsmat_42

% use model to compute log likelihood
loglik_1 = dhmm_logprob(data_1, prior_12, transmat_12, obsmat_12)
loglik_2 = dhmm_logprob(data_2, prior_22, transmat_22, obsmat_22)
loglik_3 = dhmm_logprob(data_3, prior_32, transmat_32, obsmat_32)
loglik_4 = dhmm_logprob(data_4, prior_42, transmat_42, obsmat_42)

% use model to clasify giving new data
data_new1= [2   1   2   1   1   1   2   1   1   2   2   2   2   2   1   1   2   1
1   2   2   1   1   1   2   2   2   1   2   2
];
loglik_1new1 = dhmm_logprob(data_new1, prior_12, transmat_12, obsmat_12)
loglik_2new1 = dhmm_logprob (data_new1, prior_22, transmat_22, obsmat_22)
loglik_3new1 = dhmm_logprob(data_new1, prior_32, transmat_32, obsmat_32)
loglik_4new1 = dhmm_logprob(data_new1, prior_42, transmat_42, obsmat_42)


data_new2 = [3  4   4   4   3   4   4   4   4   4   3   4   4   4   3   4   4   4
3   4   4   4   4   4   3   4   4   3   3   4];
loglik_1new2 = dhmm_logprob(data_new2, prior_12, transmat_12, obsmat_12)
loglik_2new2 = dhmm_logprob (data_new2, prior_22, transmat_22, obsmat_22)
loglik_3new2 = dhmm_logprob(data_new2, prior_32, transmat_32, obsmat_32)
loglik_4new2 = dhmm_logprob(data_new2, prior_42, transmat_42, obsmat_42)

data_new3 = [6  6   5   5   5   5   5   6   6   5   6   6   6   6   5   5   6   6
5   6   6   6   6   6   6   6   6   6   6   6];
loglik_1new3 = dhmm_logprob(data_new3, prior_12, transmat_12, obsmat_12)
loglik_2new3 = dhmm_logprob (data_new3, prior_22, transmat_22, obsmat_22)
loglik_3new3 = dhmm_logprob(data_new3, prior_32, transmat_32, obsmat_32)
loglik_4new3 = dhmm_logprob(data_new3, prior_42, transmat_42, obsmat_42)
```

```
data_new4 = [7  7   7   7   7   7   8   8   8   8   8   8   8   8   8   8   8   8
8   8   8   8   8   8   8   8   8   8   8   8];
loglik_1new4 = dhmm_logprob(data_new4, prior_12, transmat_12, obsmat_12)
loglik_2new4 = dhmm_logprob(data_new4, prior_22, transmat_22, obsmat_22)
loglik_3new4 = dhmm_logprob(data_new4, prior_32, transmat_32, obsmat_32)
loglik_4new4 = dhmm_logprob(data_new4, prior_42, transmat_42, obsmat_42)

%a HMM trained by lifetime data for prognosis
O=8;
Q=4;

prior_1 = normalise(rand(Q,1));
transmat_1 = mk_stochastic(rand(Q,Q));
obsmat_1 = mk_stochastic(rand(Q,O));

[LL, prior_2, transmat_2, obsmat_2] = dhmm_em(data_all, prior_1, transmat_1,
obsmat_1, size(data_all,1));
LL
prior_2
transmat_2
obsmat_2

loglik = dhmm_logprob(data_all, prior_2, transmat_2, obsmat_2)
```

Bibliography

Iso 13379 condition monitoring and diagnostics of machines - data interpretation and diagnostics techniques.

Iso 17359:2011, condition monitoring and diagnostics of machines - general guidelines.

Anderson, D., Jarzynski, J., and Salant, R. (2000). Condition monitoring of mechanical seals: detection of film collapse using reflected ultrasonic waves. *Proceedings of the Institution of Mechanical Engineers, Part C: Journal of Mechanical Engineering Science*, 214(9):1187–1194.

Anderson, W., Jarzynski, J., and Salant, R. (2002). Monitoring the condition of liquid-lubricated mechanical seals. *Sealing Technology*, 2002(2):6–11.

Bai, Y. and Bai, Q. (2012). *Subsea engineering handbook*. Gulf Professional Publishing.

Baum, L. E., Eagon, J. A., et al. (1967). An inequality with applications to statistical estimation for probabilistic functions of markov processes and to a model for ecology. *Bull. Amer. Math. Soc*, 73(3):360–363.

Bencomo, A. (2012). Applications of condition monitoring for the subsea industry.

Campen, C. H., Matos, J. L., and Roncace, J. (2009). Subsea multiphase pumping systems. US Patent 7,569,097.

D. Mewes, G. Aleksieva, A. S. A. L. (2008). Modelling twin-screw multiphase pumps - a realistic approach to determine the entire performance behaviour.

Dempster, A. P., Laird, N. M., and Rubin, D. B. (1977). Maximum likelihood from incomplete data via the em algorithm. *Journal of the royal statistical society. Series B (methodological)*, pages 1–38.

Dong, M. and He, D. (2007). A segmental hidden semi-markov model (hsmm)-based diagnostics and prognostics framework and methodology. *Mechanical Systems and Signal Processing*, 21(5):2248–2266.

Donnelly, J. (2013). Condition and performance monitoring of subsea production systems.

Dragomir, O. E., Gouriveau, R., Dragomir, F., Minca, E., and Zerhouni, N. (2009). Review of prognostic problem in condition-based maintenance. In *European Control Conference, ECC'09.*, pages 1585–1592.

Dwyer-Joyce, R., Drinkwater, B., and Donohoe, C. (2003). The measurement of lubricant–film thickness using ultrasound. *Proceedings of the Royal Society of London. Series A: Mathematical, Physical and Engineering Sciences*, 459(2032):957–976.

Egashira, K., Shoda, S., Tochikawa, T., Furukawa, A., et al. (1998). Backflow in twin-screw-type multiphase pump. *SPE production & facilities*, 13(01):64–69.

Eriksson, K. (2010). Control system and condition monitoring for a subsea gas compressor pilot. In *Control 2010, UKACC International Conference on*, pages 1–6. IET.

Eriksson, K., Antonakopoulos, K., et al. (2014). Subsea processing systems: Optimising the maintenance, maximising the production. In *Offshore Technology Conference-Asia*. Offshore Technology Conference.

Evans, J. G. and Janssen, S. (2002). Developments in sealing technology within multiphase pumps. In *Nineteenth International Pump Users Symposium, Turbomachinery Laboratory, Texas A&M University, College Station, Texas*, pages 25–32.

Feng, C., Yueyuan, P., Ziwen, X., and Pengcheng, S. (2001). Thermodynamic performance simulation of a twin-screw multiphase pump. *Proceedings of the Institution of Mechanical Engineers, Part E: Journal of Process Mechanical Engineering*, 215(2):157–163.

Friedemann, J. D., Varma, A., Bonissone, P., Iyer, N., et al. (2008). Subsea condition monitoring–a path to increased availability and increased recovery. In *Intelligent Energy Conference and Exhibition*. Society of Petroleum Engineers.

Gao, T.-y., Yang, D.-f., Cao, F., and Jiao, J.-c. (2011). Temperature and thermodynamic deformation analysis of the rotors on a twin screw multiphase pump with high gas volume fractions. *Journal of Zhejiang University SCIENCE A*, 12(9):720–730.

Heng, A., Zhang, S., Tan, A. C., and Mathew, J. (2009). Rotating machinery prognostics: State of the art, challenges and opportunities. *Mechanical Systems and Signal Processing*, 23(3):724–739.

Holenstein, A., Milek, J., and Birchler, B. (2000). Method for monitoring the condition of a mechanical seal. US Patent 6,065,345.

Huang, Z. P., Zhang, Z., Zhang, J. K., Chen, K., Fu, P., and Lin, Z. B. (2014). Research on the micro scope condition of end face of liquid-lubricated mechanical seals. *Advanced Materials Research*, 898:574–577.

Jardine, A., Joseph, T., and Banjevic, D. (1999). Optimizing condition-based maintenance decisions for equipment subject to vibration monitoring. *Journal of Quality in Maintenance Engineering*, 5(3):192–202.

Kim, J.-H., Lee, H.-C., Kim, J.-H., Choi, Y.-S., Yoon, J.-Y., Yoo, I.-S., and Choi, W.-C. (2015). Improvement of hydrodynamic performance of a multiphase pump using design of experiment techniques. *Journal of Fluids Engineering*, 137(8):081301.

Klein, O. and Hoffmeister, H. (2008). Corrosive, erosive and abrasive wear in twin screw multiphase pumps. In *Evolving Multiphase Boosting Technology Conference paper Hannover, Deutschland*.

Lagnebäck, R. (2007). *Evaluation of wayside condition monitoring technologies for condition-based maintenance of railway vehicles*. Luleå University of Technology Luleå.

Langli, G., Masdal, S., Nyhavn, F., Carlsen, I., et al. (2001). Ensuring operability and availability of complex deepwater subsea installations: A case study. In *ANNUAL OFFSHORE TECHNOLOGY CONFERENCE*, volume 1, pages 587–602. Offshore Technology Conference.

Le, T. T., Berenguer, C., and Chatelain, F. (2014a). Multi-branch hidden semi-markov modeling for rul prognosis.

Le, T. T., Chatelain, F., and Berenguer, C. (2014b). Hidden markov models for diagnostics and prognostics of systems under multiple deterioration modes. In *European Safety and Reliability Conference-ESREL 2014*, pages 1197–1204. Taylor & Francis-CRC Press/Balkema.

Lin, D., Wiseman, M., Banjevic, D., and Jardine, A. K. (2004). An approach to signal processing and condition-based maintenance for gearboxes subject to tooth failure. *Mechanical Systems and Signal Processing*, 18(5):993–1007.

Mba, D., Roberts, T., Taheri, E., and Roddis, A. (2006). Application of acoustic emission technology for detecting the onset and duration of contact in liquid lubricated mechanical seals. *Insight-Non-Destructive Testing and Condition Monitoring*, 48(8):486–487.

Murphy, K. (2005). Hidden markov model (hmm) toolbox for matlab.

Prang, A. J. and Cooper, P. (2004). Enhanced multiphase flow predictions in twin-screw pumps. In *Proceedings of the 21st International Pump User Symposium, Baltimore, MD, March*, pages 8–11.

Qiu, H., Liao, H., and Lee, J. (2005). Degradation assessment for machinery prognostics using hidden markov models. In *ASME 2005 International Design Engineering Technical Conferences and Computers and Information in Engineering Conference*, pages 531–537. American Society of Mechanical Engineers.

Rausand, M. (2013). *Risk assessment: Theory, methods, and applications*, volume 115. John Wiley & Sons.

Reddyhoff, T., Dwyer-Joyce, R., and Harper, P. (2006). Ultrasonic measurement of film thickness in mechanical seals. *Sealing Technology*, 2006(7):7–11.

Rohlfing, G. (2010). Condition monitoring of multiphase pumps. *World Pumps*, 2010(4):34–39.

Ruan, B., Salant, R. F., and Green, I. (1997). A mixed lubrication model of liquid/gas mechanical face seals. *Tribology transactions*, 40(4):647–657.

Ruddy, A., Dowson, D., and Taylor, C. (1982). The prediction of film thickness in a mechanical face seal with circumferential waviness on both the face and the seat. *Journal of Mechanical Engineering Science*, 24(1):37–43.

Rus, T., Dular, M., Širok, B., Hočevar, M., and Kern, I. (2007). An investigation of the relationship between acoustic emission, vibration, noise, and cavitation structures on a kaplan turbine. *Journal of Fluids Engineering*, 129(9):1112–1122.

Salant, R. F. and Cao, B. (2005). Unsteady analysis of a mechanical seal using duhamels method. *Journal of tribology*, 127(3):623–631.

Scharf, A., R. T. V. T. A. G. R. M. R. G. M. D. (2006). Performance and application range of multiphase twin-screw pumps with declining pitch.

Schoener, H.-J. (2004). Multiphase pumping - a successfully growing oil field production technology. *S C A N D I N A V I A N O I L - G A S M A G A Z I N E*.

Scott, S. L., Devegowda, D., and Martin, A. M. (2004). Assessment of subsea production and well systems. *Department of Petroleum Engineering, Texas A&M University, Final Report Submitted to the US Department of Interior–Minerals Management Service (MMS), Technology Assessment & Research (TA&R) Program.*

Si, X.-S., Wang, W., Hu, C.-H., and Zhou, D.-H. (2011). Remaining useful life estimation–a review on the statistical data driven approaches. *European Journal of Operational Research*, 213(1):1–14.

SINTEF (2009). *OREDA Offshore Reliability Data 5th Edition.*

Vetter, G., Wirth, W., Korner, H., and Pregler, S. (2000a). Multiphase pumping with twin-screw pumps-understand and model hydrodynamics and hydroabrasive wear. In *PROCEEDINGS OF THE INTERNATIONAL PUMP USERS SYMPOSIUM*, pages 153–170.

Vetter, G., Wirth, W., Korner, H., and Pregler, S. (2000b). Multiphase pumping with twin-screw pumps-understand and model hydrodynamics and hydroabrasive wear. In *PROCEEDINGS OF THE INTERNATIONAL PUMP USERS SYMPOSIUM*, pages 153–170.

Viterbi, A. J. (1967). Error bounds for convolutional codes and an asymptotically optimum decoding algorithm. *Information Theory, IEEE Transactions on*, 13(2):260–269.

Wang, W., Scarf, P., and Smith, M. (2000). On the application of a model of condition-based maintenance. *Journal of the Operational Research Society*, pages 1218–1227.

Yamauchi, Y. and Inoue, K. (1994). Method for predicting abnormality of mechanical seal and apparatus for predicting same. US Patent 5,345,829.

You, M., Liu, F., and Meng, G. (2011). Benefits from condition monitoring techniques: a case study on maintenance scheduling of ball grid array solder joints. *Proceedings of the Institution of Mechanical Engineers, Part E: Journal of Process Mechanical Engineering*, page 2041300910393426.

Zhang, Z., Chen, K., Zhang, E. Q., and Fu, P. (2014). Mechanical seal condition monitoring technology research. In *Applied Mechanics and Materials*, volume 529, pages 344–348. Trans Tech Publ.

Curriculum Vitae

Name:	**Fenfen Liu**	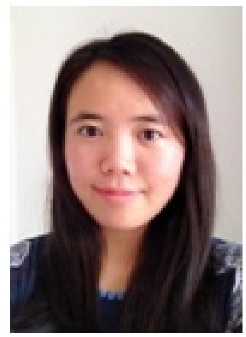
Gender:	Female	
Date of birth:	9. July 1989	
Address:	Herman Kragsvei 39-41, 7050 Trondheim	
Nationality:	Chinese	
Email (1):	fenfenl@stud.ntnu.no	
Email (2):	soregara@gmail.com	
Telephone:	+47 94431451	

Language Skills

English: Fluent in speaking and writing

Norwegian: Level 2

Japanese: Level N2 of the Japanese-Language Proficiency Test

Education

- Norwegian University of Science and Technology (NTNU)

  Degree: Master of Science

  RAMS Engineering (Reliability, Availability, Maintainability and Safety)

  Specialization: Maintenance Optimization - Condition Based Maintenance (CBM)

- Tongji University (Shanghai, China)

  Degree: Bachelor of Engineering

Vehicle Engineering (Railway)

Thesis: Design of High-frequency Signal Generator based on FPGA

Computer Skills

- Analyzing: CARA FaultTree, MATLAB, ANSYS, MiniTab, Protel 99
- Mapping: Auto CAD, CATIA, Photoshop
- Programming: Quartus II, Signal TAP II, ASP.NET, C++, Verilog HDL

Experience

- 08/2014–12/2014 Student Assistant (TPK5115 Risk Management in Project)
  NTNU(Norwegian University of Science and Technology), Trondheim (Norway)
  - help students to solve their problems about the course;
  - grade students' exercises;
  - bridge the communication between lecturer and students.

- 07/2011–05/2013 Maintenance Engineer
  Guangzhou Metro Corporation (China)
  - maintenance of cranes, compressors, Automatic Train Washing Machine, Rack Cart Machine, Automatic Stereoscopic Warehouse, etc.
  - scheduled maintenance planning and carried out corrective maintenance;
  - compiled maintenance procedures and regulations;
  - asset management: updated all relevant information for all equipment, recorded the downtime and failure rate for each machine;
  - spare parts management: tracked the replacement interval for each spare, checked the number of stored spare parts, and purchased new spares;

Hobbies and Other Activities

- Winner of the Student Choice Award of YOUREXTREM 2014 Competition hosted by Kongsberg Gruppen(2014)
- Volunteer of Trondheim Kammer Musikk Festival (2013-2014)
- Chinese Collaborator of Coralua Trondheim International Choir Festival (2014)
- Social Survey of Caring for the Disadvantaged in Society (2009)
- Social Survey of Housing Status and Needs of White-collars in China (2008)

Hobbies: Hiking, cycling, skiing, ice skating, ball sports, travelling, reading, listening music, cooking, baking, etc.